

AD-A045 127

COLD REGIONS RESEARCH AND ENGINEERING LAB HANOVER N H F/G 13/9
MECHANICS OF CUTTING AND BORING. PART 6. DYNAMICS AND ENERGETIC--ETC(U)
AUG 77 M MELLOR

UNCLASSIFIED

CRREL-77-19

NL

| OF |
AD
A045127



END
DATE
FILMED
11 -77
DDC

CRREL

REPORT 77-19

Handwritten scribble (12)

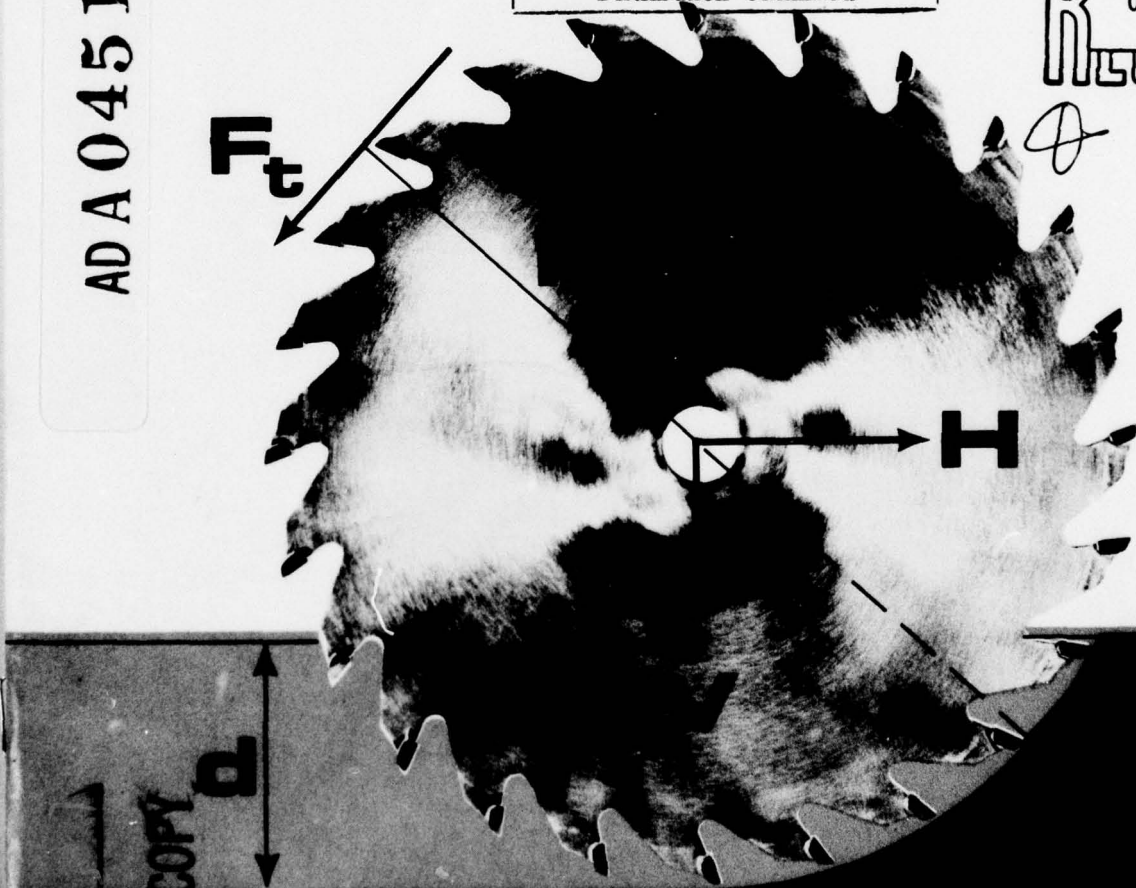


Mechanics of cutting and boring *Part VI: Dynamics and energetics of* *transverse rotation machines*

AD A 045 127

DISTRIBUTION STATEMENT A
Approved for public release;
Distribution Unlimited

DDC
RECEIVED
OCT 14 1977
B



COPIES

CRREL Report 77-19

Mechanics of cutting and boring *Part VI: Dynamics and energetics of* *transverse rotation machines*

Malcolm Mellor

August 1977

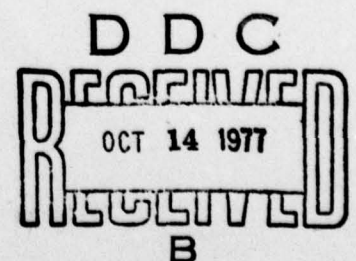
Prepared for

**DIRECTORATE OF FACILITIES ENGINEERING
OFFICE, CHIEF OF ENGINEERS**

By

**CORPS OF ENGINEERS, U.S. ARMY
COLD REGIONS RESEARCH AND ENGINEERING LABORATORY
HANOVER, NEW HAMPSHIRE**

Approved for public release; distribution unlimited.



Unclassified

SECURITY CLASSIFICATION OF THIS PAGE (When Data Entered)

REPORT DOCUMENTATION PAGE		READ INSTRUCTIONS BEFORE COMPLETING FORM
1. REPORT NUMBER 14 CRREL Report 77-19	2. GOVT ACCESSION NO.	3. RECIPIENT'S CATALOG NUMBER
4. TITLE (and Subtitle) MECHANICS OF CUTTING AND BORING Part 6: Dynamics and Energetics of Transverse Rotation Machines		5. TYPE OF REPORT & PERIOD COVERED
7. AUTHOR(s) 20 Malcolm Mellor		6. PERFORMING ORG. REPORT NUMBER
9. PERFORMING ORGANIZATION NAME AND ADDRESS U.S. Army Cold Regions Research and Engineering Laboratory Hanover, New Hampshire 03755		8. CONTRACT OR GRANT NUMBER(s) 16
11. CONTROLLING OFFICE NAME AND ADDRESS Directorate of Facilities Engineering Office, Chief of Engineers Washington, D.C. 20314		10. PROGRAM ELEMENT, PROJECT, TASK AREA & WORK UNIT NUMBERS DA Project 4A762719AT42 Technical Area 02 Work Unit 004 12
14. MONITORING AGENCY NAME & ADDRESS (if different from Controlling Office)		12. REPORT DATE August 1977
		13. NUMBER OF PAGES 43 12 45p.
		15. SECURITY CLASS. (of this report) Classified
		16. DECLASSIFICATION/DOWNGRADING SCHEDULE
16. DISTRIBUTION STATEMENT (of this Report) Approved for public release; distribution unlimited. pt 4 A040 760		
17. DISTRIBUTION STATEMENT (of the abstract entered in Block 20, if different from Report)		
18. SUPPLEMENTARY NOTES		
19. KEY WORDS (Continue on reverse side if necessary and identify by block number) Boring machines Machine design Excavating machines Permafrost excavation Excavation Rock cutting Ice cutting		
20. ABSTRACT (Continue on reverse side if necessary and identify by block number) The report deals with forces and power levels in cutting machines having a disc or drum that rotates about an axis perpendicular to the direction of advance. The forces on individual cutting tools are related to position on the rotor and to characteristics such as tool layout, rotor speed, rotor size, machine advance speed, and rotor torque. Integration leads to expressions for force components acting on the rotor axis, taking into account tool characteristics, cutting depth of the rotor, and rotor torque. These provide estimates of tractive thrust and thrust normal to the primary free surface. For self-propelled machines, this leads to considerations of traction, normal reaction, weight and balance, and power/weight ratios. Specific energy consumption is analyzed and related to machine		

037 100

over
lpg

SECURITY CLASSIFICATION OF THIS PAGE(When Data Entered)

20. Abstract (cont'd)

characteristics and strength of the material being cut. Power per unit working area is discussed, and data for existing machines are summarized. Power requirements for ejection of cuttings are analyzed, and the hydrodynamic resistance on underwater cuttings is treated. A number of worked examples are given to illustrate the principles discussed in the report.

ACCESSION for		
NTIS	White Section	<input checked="" type="checkbox"/>
DDC	Buff Section	<input type="checkbox"/>
UNANNOUNCED		<input type="checkbox"/>
JUSTIFICATION		
BY		
DISTRIBUTION/AVAILABILITY CODES		
Dist.	AVAIL and/or	SPECIAL
A		

SECURITY CLASSIFICATION OF THIS PAGE(When Data Entered)

PREFACE

This report was prepared by Dr. Malcolm Mellor, Physical Scientist, Experimental Engineering Division, U.S. Army Cold Regions Research and Engineering Laboratory. The work was done under DA Project 4A762719AT42, *Design, Construction and Operations Technology for Cold Regions*, Technical Area 02, *Soils and Foundations Technology*, Work Unit 004, *Excavation in Frozen Ground*.

The author is grateful to Paul V. Sellmann for his continued interest, especially in asking — and answering — awkward questions. Technical review of the manuscript was provided by Mr. Sellmann and Dr. Haldor Aamot of CRREL, and by Dr. Ivor Hawkes.

The contents of this report are not to be used for advertising or promotional purposes. Citation of brand names does not constitute an official endorsement or approval of the use of such commercial products.

CONTENTS

	Page
Abstract	i
Preface	iii
Foreword	vi
Introduction	1
Terminology	2
Forces on individual cutters	3
Torque force and tool force	6
Forces on the rotor axis	8
Tractive thrust and down thrust	12
Alternative tool force formulations	15
Vehicle traction	16
Power/weight ratio	17
Weight and balance	19
Force, torque, speed and power	19
Specific energy	20
Efficiency and performance index	23
Power density	24
Power requirements for ejection of cuttings	26
Hydrodynamic resistance in underwater cutting	27

ILLUSTRATIONS

Figure		Page
1. Definition of symbols		2
2. Variation of tool force f_{θ} with angular position θ for different numbers of tracking cutters		5
3. Simple layout of cutters along n helices		7
4. Variation of $(f_{\theta})_{\max}$ with cutting depth d		9
5. Variation of axle force components H and V with cutting depth d , assuming constant torque		11
6. Variation of axle force components H and V with K , assuming constant torque and tool force components proportional to ℓ		14
7. Examples of minimum weight requirements for a carrier vehicle as functions of cutting depth		18
8. Total installed power plotted against gross machine weight for a variety of existing machines		18
9. Moments affecting the balance of a mobile machine		19
10. Volumetric cutting rate per unit power as a function of specific energy		22
11. Variation of maximum traverse speed with cutting depth when E_s is held constant		22
12. Plot of E_s against σ_c made from performance records of various existing machines		23
13. Usable rotor power plotted against the area of one quadrant of the rotor for various existing machines		25

MECHANICS OF CUTTING AND BORING

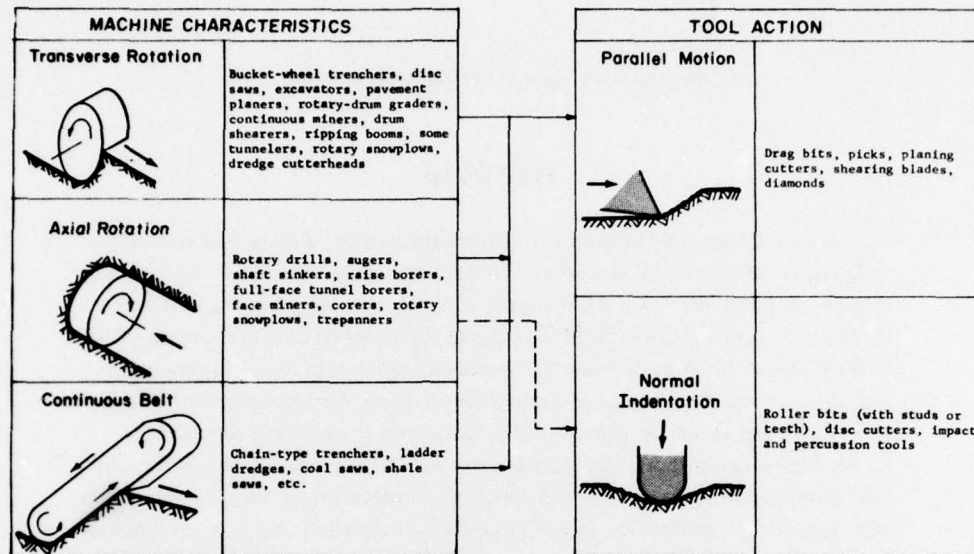
FOREWORD

There are a multitude of tasks that involve the cutting, drilling, or excavating of natural ground materials and massive structural materials. The required technology varies with the properties of the materials and with the scale of operations, but a broad distinction can be made on the basis of the strength, cohesion, and ductility of the material that is to be worked. In weak materials that have little cohesion (e.g. typical soils) the forces and energy levels required for separation and disaggregation are often small compared with the forces and energy levels required for acceleration and transport, and materials handling technology dominates the consideration. By contrast, in strong materials that exhibit brittle fracture characteristics (e.g. rock, concrete, ice, frozen ground) the forces and energy levels required for cutting and breaking are high compared with those required for handling the broken material, and the technical emphasis is on cutting and breaking processes.

CRREL has long been concerned with excavating and drilling in ice and frozen ground, and over the past decade systematic research has been directed to this technical area. The research has covered a wide range of established technologies and novel concepts but, for short term applications, interest has necessarily centered on special developments of proven concepts. In particular, there has been considerable concern with direct mechanical cutting applied to excavation, cutting, and drilling of frozen soils, glacier ice, floating ice, and dense snow. During the course of this work, numerous analyses and design exercises have been undertaken, and an attempt is now being made to develop a systematic analytical scheme that can be used to facilitate future work on the mechanics of cutting and boring machines.

In the industrial sector, rock-cutting machines are usually designed by applying standard engineering methods in conjunction with experience gained during evolution of successive generations of machines. This is a very sound approach for gradual progressive development, but it may not be appropriate when there are requirements for rapid development involving radical departures from established performance characteristics, or for operations in unusual and unfamiliar materials. A distinct alternative is to design more or less from first principles by means of theoretical or experimental methods, but this alternative may not be practically feasible in its more extreme form.

There are numerous difficulties in attempting a strict scientific approach to the design of rock-cutting machines. The relevant theoretical rock mechanics is likely to involve controversial fracture theories and failure criteria, and to call for detailed material properties that are not normally available to a machine designer. Direct experiments are costly and time-consuming, and experimental data culled from the literature may be unsuitable for extrapolation, especially when (as is sometimes the case) they are described by relationships that violate the basic physics of the problem. Comprehensive mechanical analyses for rock-cutting machines have not yet



Classification of machines and cutting tools for analytical purposes.

evolved, and while established design principles for metal-cutting machine tools may be helpful, they do not cover all pertinent aspects. For example, there are usually enormous differences in forces and power levels between machine tools and excavating machines, and force components that can be almost ignored in a relatively rigid machine tool may be crucial design factors for large mobile rock cutters that are highly compliant.

In dealing with cold regions problems where neither outright empiricism nor highly speculative theory seem appropriate, some compromise approaches have been adopted. While simple and practical, these methods have proved useful for analysis and design of cutting and boring machines working under a wide range of conditions in diverse materials, and it seems possible that they might form the basis for a general analytical scheme. The overall strategy is to examine the kinematics, dynamics and energetics for both the cutting tool and the complete machine according to a certain classification, adhering as far as possible to strict mechanical principles, but holding to a minimum the requirements for detailed information on the properties of the material to be cut.

Kinematics deals with the inherent relationships defined by the geometry and motion of the machine and its cutting tools, without much reference to the properties of the material being cut. *Dynamics* deals with forces acting on the machine and its cutting tools, taking into account machine characteristics, operating procedures, wear effects, and material properties. *Energetics* deals largely with specific energy relationships that are determined from power considerations involving forces and velocities in various parts of the system, taking into account properties of the materials that are being cut.

These mechanical principles are applied in accordance with a classification based on the characteristic motions of the major machine element and the actual cutting

tools, as illustrated above. Machines are classified as *transverse rotation*, *axial rotation*, or *continuous belt*, while the action of cutting tools is divided into *parallel motion* and *normal indentation*.

Transverse rotation devices turn about an axis that is perpendicular to the direction of advance, as in circular saws. The category includes such things as bucket-wheel trenchers and excavators, pavement planers, rotary-drum graders, large disc saws for rock and concrete, certain types of tunneling machines, drum shearers, continuous miners, ripping booms, some rotary snowplows, some dredge cutter-heads, and various special-purpose saws, millers and routers. *Axial rotation* devices turn about an axis that is parallel to the direction of advance, as in drills. The category includes such things as rotary drills, augers and shaft-sinking machines, raise borers, full-face tunnel boring machines, corers, trepanners, some face miners, and certain types of snowplows. *Continuous belt* machines represent a special form of transverse rotation device, in which the rotor has been changed to a linear element, as in a chain saw. The category includes "digger chain" trenchers, ladder sledges, coal saws, shale saws, and similar devices.

In tool action, *parallel motion* denotes an active stroke that is more or less parallel to the surface that is being advanced by the tool, i.e. a planing action. Tools working this way include drag bits for rotary drills and rock-cutting machines; picks for mining and tunneling machines; teeth for ditching and dredging buckets; trencher blades; shearing blades for rotary drills, surface planers, snowplows, etc.; diamond edges for drills and wheels; and other "abrasive" cutters. *Normal indentation* denotes an active stroke that is more or less normal to the surface that is being advanced, i.e. one which gives a pitting or cratering effect such as might be produced by a stone chisel driven perpendicular to the surface. Tools working this way include roller rock bits for drills, tunneling machines, raise borers, reamers, etc.; disc cutters for tunneling machines; and percussive bits for drills and impact breakers.

A few machines and operations do not fit neatly into this classification. For example, certain roadheaders and ripping booms used in mining sump-in by axial rotation and produce largely by transverse rotation, and there may be some question about the classification of tunnel reamers and tapered rock bits. However, the classification is very satisfactory for general mechanical analysis.

Complete treatment of the mechanics of cutting and boring is a lengthy task, and in order to expedite publication a series of reports dealing with various aspects of the problem will be printed as they are completed. The main topics to be covered in this series are:

1. Kinematics of transverse rotation machines (Special Report 226, May 1975)
2. Kinematics of axial rotation machines (CRREL Report 76-16, June 1976)
3. Kinematics of continuous belt machines (CRREL Report 76-17, June 1976)
4. Dynamics and energetics of parallel-motion tools (CRREL Report 77-7, April 1977)
5. Dynamics and energetics of normal indentation tools
6. Dynamics and energetics of transverse rotation machines
7. Dynamics and energetics of axial rotation machines
8. Dynamics and energetics of continuous belt machines.

MECHANICS OF CUTTING AND BORING
PART 6: DYNAMICS AND ENERGETICS OF TRANSVERSE ROTATION MACHINES

by

Malcolm Mellor

Introduction

This report deals with forces, torques, energy requirements and power demands in transverse-rotation cutting machines. Examples and illustrations of such machines are given in Part 1 of this series; all employ a rotary cutting unit that revolves about an axis perpendicular to the direction of advance, and virtually all machines of the class utilize parallel-motion tools as the basic cutting elements.

Kinematic factors controlled by the geometry and motion of a transverse-rotation machine are dealt with in Part 1. Cutting forces and energy requirements for parallel-motion tools are treated in Part 4, but without reference to the various types of machines on which they might be mounted. This report draws on the information of Parts 1 and 4, and goes on to develop relationships that describe the dynamics and energetics of the complete cutting system. The main emphasis is on relationships embodying simple parameters that are likely to be available to a machine designer.

The first aim is to examine the forces of individual cutting tools when they are mounted on a rotor, and then to determine how an assembly of tools affects the torque and the axle forces for the rotor as a whole. This leads to estimates of the thrust or traction requirements for the rotor carriage in terms of rotor torque, and to estimates of the required thrust or reaction in a direction normal to the traverse plane. The power/weight ratio of a machine provides some indication of the balance between power, traction and reaction, and appropriate data compilations are useful for reference. Another factor to be considered in the design of a rotor carriage is the moment developed by the cutting system, since this affects the weight and balance requirements for a mobile machine.

Energy utilization can be assessed in terms of energy consumed per unit volume of excavation, taking account of how the total energy is distributed among the various subsystems and sources of loss. As a practical matter, work and energy are usually accounted for in terms of rate of working or power, and specific energy is obtained by relating power to volumetric excavation rate. Energetic efficiency can be examined further by comparing specific energy with the strength of the work material, the intention being to obtain a dimensionless index of performance that compares behavior of different machines in the same material or, alternatively, behavior of a given machine in different materials. Another useful parameter for comparing machines is the power density of the cutting element, defined as the power applied per unit area of the cutting surface.

Finally, estimates have to be made for the power that goes into accelerating and ejecting cuttings and, if the machine is to be operated underwater, into overcoming fluid drag on all the rotor surfaces.

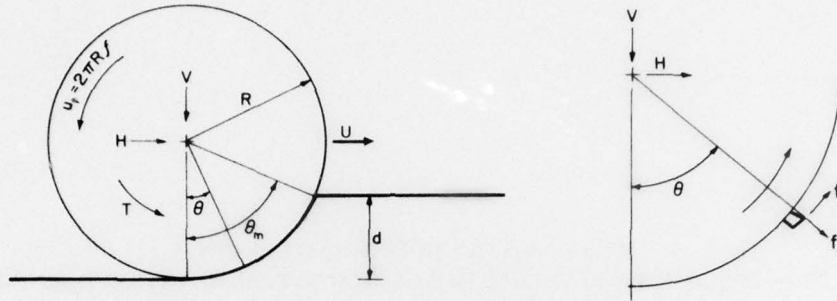


Figure 1. Definition of symbols.

Terminology

Some of the terminology used in this report has already been listed in Parts 1 and 4. Additional terms are given below.

Tool forces, or cutter forces, are the forces developed by the individual cutting tools during the cutting process. The resultant force on a tool can be resolved into tangential and radial components f_θ and f_R with respect to the rotor on which they are mounted (Fig. 1). These components correspond approximately to the tangential and normal components f_t and f_n that are discussed in Part 4. Since the chipping depth l varies systematically through the working sweep on a transverse-rotation machine, f_θ and f_R are functions of angular position θ . If a tool is symmetrical in the sense that side rakes are equal (or zero), there is not likely to be a significant side component f_s (orthogonal to f_θ and f_R), but there is some possibility of a finite f_s when a tool is working parallel to a relieving kerf, as discussed in Part 4.

The *ratio of tool force components* K is f_R/f_θ , i.e. the ratio of the radial component to the tangential component. It is the tangent of the angle between the resultant cutting force and the tangential direction. In practical terms, it gives a measure of the sharpness of the tool, with high values of K indicating blunt or worn tools. For most purposes in this report, K is assumed to be invariant with the chipping depth of the tool.

Rotor cutting torque T is the net torque developed by the rotary cutting unit when it applies tangential cutting forces to the tool tips at constant speed. The externally applied torque required to overcome bearing friction, gear or transmission losses, and windage (or fluid resistance when cutting underwater) is not normally included, nor is the torque required to accelerate the rotor. In some circumstances it is not possible to separate cutting forces from the tangential forces required to accelerate chips or cuttings, and so the net rotor torque will often include the effects of chip ejection.

Torque force F_t is the tangential force given by $F_t = T/R$, where R is the radius of the rotor to the tool tips. At any instant it is equal to the sum of the tangential cutting forces f_θ that are being applied at radius R by all the active tools.

Axle forces on the rotor are the forces developed on the axle by the cutting process. The resultant axle force at any instant is given by a summation of the vector cutting forces on all the active tools. The resultant axle force can be resolved into orthogonal components that are: 1) parallel to the direction of advance, 2) normal to the primary free surface, and 3) parallel to the rotor axis. The component parallel to the rotor axis should be zero for a symmetrical rotor that is dynamically balanced about the mid-section. The component parallel to the direction of advance

H , which is often horizontal, equals the sum of the components of f_θ and f_R resolved in that direction. The component normal to the primary free surface V , which is often vertical, equals the sum of the components of f_θ and f_R resolved in the same normal direction.

The *tractive thrust* of a machine is the force developed parallel to the direction of advance in order to overcome cutting resistance. It equals the axle force component H . When the rotary cutting unit is mounted on a self-propelled vehicle, the tractive thrust is the net forward force developed by the wheels or crawler tracks, i.e. the "drawbar pull."

The *down thrust* of a machine, which may be positive or negative, is the force perpendicular to the traverse direction that is required to maintain the rotary cutting unit at the required operating depth. It is equal to the axle force component V . When the rotary cutting unit is mounted on a self-propelled vehicle, the available down thrust is limited by the weight and balance of the machine.

Machine power P can be partitioned broadly as rotor power P_R , thrust power P_H , and power loss P_L . The *rotor power* is the power consumed by the rotor for cutting, i.e. $P_R = \omega T = 2\pi f T = 2\pi R f F_t$, where ω and f are angular velocity and angular frequency respectively. The *thrust power* is the net power used to overcome cutting resistance in the direction of advance, i.e. $P_H = UH$, where U is the advance speed of the machine. The *power loss* is the power that does not contribute directly to the cutting process. Power loss could include power used in windmilling the rotor against bearing friction and air resistance or water resistance. It could include transmission losses (mechanical, hydraulic or electrical) in the rotor drive and/or the vehicle drive train. It could also include power consumed in overcoming external track or wheel resistance on the carrier vehicle, or in recycling cuttings on the rotor. For present purposes, power loss can also be used as a catchall to include power consumed in other necessary functions that are not directly contributing to the cutting process, e.g. conveyors, actuators, lighting, fans, sprays.

The *power density* of a cutting rotor is a term used here to denote the rotor power per unit area of cutting surface, i.e. power density Q is $P_R/R\theta_m B$, where $\theta_m = \cos^{-1} [1 - (d/R)]$ and B is rotor width. Since θ_m is normally an operating variable, an arbitrary definition of *nominal power density* is taken as a basis for comparison of machines; making $\theta_m = \pi/2$, nominal power density is $2P_R/\pi RB$.

The *specific energy* of a cutting machine is the energy consumed per unit volume of material removed. Alternatively, it is the power consumption divided by the volumetric removal rate. The *overall specific energy* for a complete machine is based on the total machine power, i.e. it is $P/\dot{v} = (P_R + P_H + P_L)/\dot{v}$ where \dot{v} is the volumetric excavation rate. The *process specific energy* for cutting is based on the actual power used for the cutting process, i.e. it is $(P_R + P_H)/\dot{v}$.

Forces on individual cutters

Each cutting tool on a rotor develops a cutting force that is determined mainly by tool geometry, rock properties and operating conditions, especially chipping depth, as described in Part 4 of this series. The cutting force can be resolved into radial and tangential components f_R and f_θ (Fig. 1); these are approximately equivalent to the normal and tangential components f_n and f_t that were discussed in Part 4, provided that U/u_t is small. For a particular type of tool working in a given isotropic material, f_R and f_θ are functions of chipping depth l ; as a general approximation, they can be expressed as

$$f_R = k_R (l/r)^a \quad (1)$$

$$f_\theta = k_\theta (l/r)^b \quad (2)$$

$$f_R/f_\theta = k_R/k_\theta (\ell/r)^{a-b} \quad (3)$$

where k_R and k_θ are proportionality constants with dimensions of force (embodying effects of tool geometry and rock properties), r is the radius of curvature of the tool tip (used here only as a normalizing constant to make ℓ dimensionless), and a and b are dimensionless exponents. Some characteristics of a and b can be deduced from the data compiled in Part 4. These data show force components either proportional to ℓ , or approximately proportional to some fractional power of ℓ . They also show f_n/f_t (i.e. f_R/f_θ) decreasing slowly with increase of ℓ , from a value that is approximately equal to unity when ℓ is small, i.e. $f_R/f_\theta \approx 1$ when $\ell \leq r$. Hence it might be reasoned that

$$a < 1 \quad b < 1$$

$$a < b$$

$$a \approx b.$$

The chipping depth ℓ is a function of the rotational frequency of the rotor f , the forward travel speed U , the number of tracking cutters n , and the angular position θ (see Part 1):

$$\ell = \frac{U}{fn} \sin \theta. \quad (4)$$

Thus, for a given set of operating conditions, the chipping depth of each individual tool increases in proportion to $\sin \theta$. With a typical upmilling rotor, the variation is from practically zero at the point of entry, up to a maximum that occurs at the point of exit when $\theta_{\max} < \pi/2$, and at $\theta = \pi/2$ when $\theta_{\max} > \pi/2$.

To simplify the discussion of tool force variations during the course of one rotor revolution, assume that $a = b = 1$, i.e. assume that cutting forces are directly proportional to chipping depth (this is a realistic assumption for some conditions – see Part 4). Under this assumption

$$f_R = k_R \frac{\ell}{r} = \frac{k_R}{r} \frac{U}{fn} \sin \theta \quad (5)$$

$$f_\theta = k_\theta \frac{\ell}{r} = \frac{k_\theta}{r} \frac{U}{fn} \sin \theta \quad (6)$$

$$\frac{f_R}{f_\theta} = \frac{k_R}{k_\theta} = K. \quad (7)$$

Since f_R and f_θ are proportional, it is only necessary to treat one component; f_θ is selected, as it relates directly to the torque of the rotor.

Consider first the situation where there is only one cutting tool on a "thin" rotor of radius R , i.e. $n = 1$ (Fig. 2a). The tangential tool force varies as

$$f_\theta = \frac{k_\theta}{r} \frac{U}{f} \sin \theta. \quad (8)$$

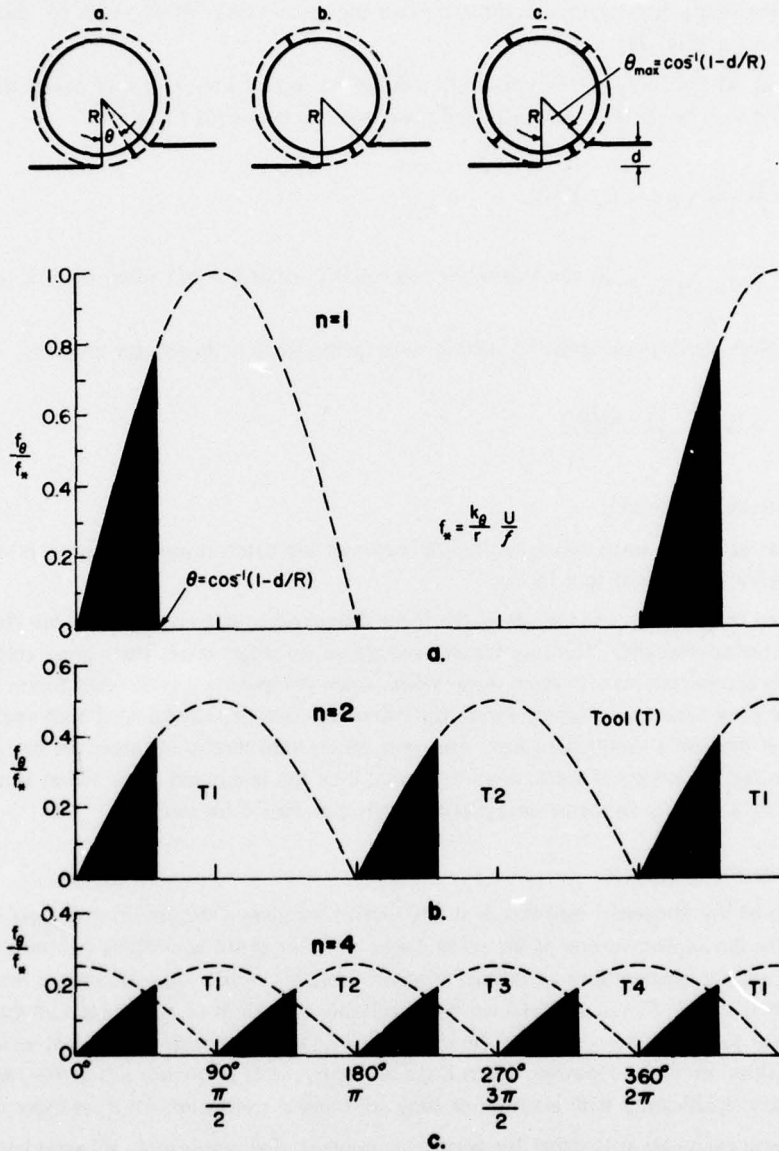


Figure 2. Variation of tool force f_{θ} with angular position θ for different numbers of tracking cutters (assuming f_{θ} proportional to ϱ).

If the rotor is slot milling, f_{θ} rises from zero at $\theta = 0$ to a maximum at $\theta = \pi/2$, before decreasing back to zero and then remaining zero for half a revolution (Fig. 2a). If the rotor is upmilling while set into the work to depth d , f_{θ} drops abruptly to zero at $\theta = \cos^{-1} [1 - (d/R)]$, as shown in Figure 2a.

Next, consider the situation where there are two diametrically opposed cutting tools, but all other conditions remain the same. This time the values of f_{θ} are only one-half the corresponding

values for the single-cutter case, but there are two tool passes through the work for each revolution of the rotor (Fig. 2b).

In general, with n tools spaced uniformly around the rotor there are n tool passes through the work for each revolution, and each tool experiences a tangential force of

$$f_{\theta} = \frac{k_{\theta}}{r} \frac{U}{nf} \sin \theta = f_{*} \frac{\sin \theta}{n} \quad (9)$$

where $f_{*} = (f_{\theta})_{\theta=\pi/2, n=1}$, i.e. the maximum tangential force at $\theta = \pi/2$ when there is only one cutter.

At any given time, the number of cutting tools in the work is the integer given by

$$\frac{\theta_m}{2\pi/n} = \frac{n \cos^{-1} [1 - (d/R)]}{2\pi} \quad (10)$$

when the residual is ignored.

The total tangential force acting on the perimeter of the rotor at any given time is the sum of the individual tangential tool forces.

So far, no mention has been made of the force fluctuations that occur as discrete chips are cut from a brittle material. The tool forces used above are mean values for a given chipping depth. It is appropriate to take such mean values when computing overall rotor forces or power levels, since peak values of chipping forces for individual tools are randomized with respect to position and time on a multi-tool rotor. However, when individual tool forces are being considered, say for the design of tools or tool mounts, then the computed mean values should be multiplied by a suitable factor to obtain peak values (see Part 4 for details).

Torque force and tool force

The sum of the tangential tool forces at any given time gives a torque force F_t that has to be overcome by the applied torque of the rotor under constant speed conditions (ignoring for the time being angular accelerations or inertial flywheel effects). When there are only a few tools on the rotor (n is small), F_t can be obtained by calculating the values of f_{θ} for each of the tools in the work and summing them, plotting the results against angular position to obtain variation of F_t with position or time. However, when there are many tools in the work together, and F_t does not vary significantly with position or time, an integral expression for F_t is more convenient.

First, some explanation is called for when it is assumed that many tools are working at a given time, since on real machines the number of tracking cutters n at any given cross section of the rotor is often three or less. Suppose that the cutters on a wide, rigid drum rotor are disposed in m rings across the width of the drum, and that there are n uniformly spaced cutters in each ring (Fig. 3). If the m rings are arranged so as to stagger systematically with respect to neighboring rings (i.e. the rings are twisted so as to set the cutters along n helices), then a side view of the drum would show mn cutters uniformly spaced around the perimeter. If the cutters are arranged to give uniform dispersion over the drum surface, as is usual, then the calculation of F_t can be based on a summation of forces for the proportion of the mn cutters that are in the work together. However, this procedure is not identical to an assumption that the rotor has mn tracking cutters, since each cutter chips to a depth that is appropriate to a ring of only n cutters.

PART 6: DYNAMICS AND ENERGETICS OF TRANSVERSE ROTATION MACHINES 7

n Cutters per revolution in each ring
 m Rings of cutters across the width of the rotor
 e.g. $n=4, m=8$

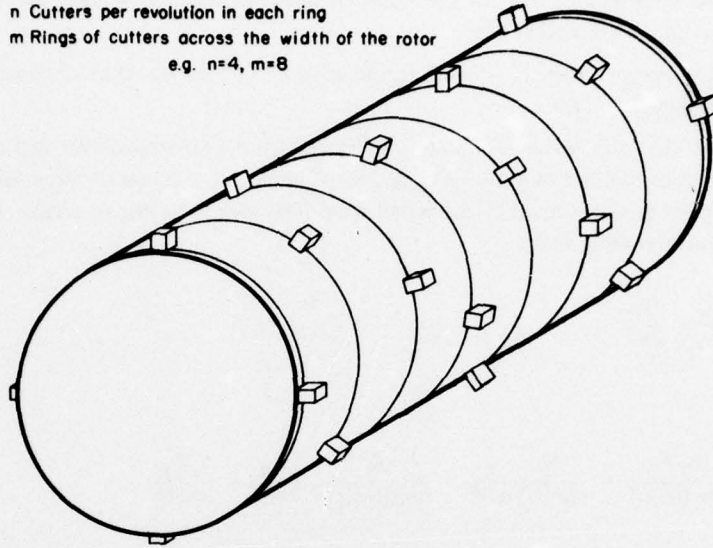


Figure 3. Simple layout of cutters along n helices.

With mn cutters spaced around the rotor, each cutter accounts for an angular interval of $2\pi/mn$, and the tangential cutting force per unit angle, f'_θ , is

$$f'_\theta = \frac{f_\theta}{2\pi/mn} \quad (11)$$

where

$$f_\theta = \frac{k_\theta}{r} \frac{U}{fn} \sin \theta = f_* \frac{\sin \theta}{n} \quad (12)$$

The total tangential force, or torque force, is thus

$$\begin{aligned} F_t &= \int_0^{\theta^m} f'_\theta d\theta = \frac{mn}{2\pi} \int_0^{\theta^m} f_\theta d\theta = \frac{mf_*}{2\pi} \int_0^{\theta^m} \sin \theta d\theta \\ &= m \frac{k_\theta}{r} \frac{U}{2\pi f} \int_0^{\theta^m} \sin \theta d\theta \end{aligned} \quad (13)$$

i.e.

$$F_t = \frac{mf_*}{2\pi} \frac{d}{R} = \frac{mk_\theta}{r} \frac{Ud}{2\pi Rf} = \frac{mk_\theta}{r} \frac{U}{u_t} d \quad (14)$$

where u_t is the tangential velocity of the rotor. It might be mentioned again that r is a constant in this context (k_θ is a function of r).

Looked at in another way, F_t is equal to the value of f_θ that would be obtained by substituting $\ell = md(U/u_t)$ in eq 6.

In principle, the rotor torque T could be estimated from a laboratory test that uses a single tool to define the relationship between f_θ and ℓ . Alternatively, the mean force for a single tool at a given angular position could be estimated from field measurements of torque T or power P_R on the rotor, recalling that

$$T = F_t R = \frac{P_R}{2\pi f} \quad (15)$$

and

$$f_\theta = \frac{\ell_\theta F_t}{md(U/u_t)} = \frac{\ell_\theta T}{md(U/u_t)R} = \frac{\ell_\theta}{md(U/u_t)} \frac{P_R}{2\pi Rf} = \frac{\ell_\theta P_R}{mdU} \quad (16)$$

It is also instructive to express f_θ as

$$f_\theta = \frac{2\pi R}{nm d} \sin \theta F_t = \frac{2\pi \sin \theta T}{nm d} = \frac{P_R \sin \theta}{nm d f} \quad (17)$$

For $d/R < 1$, maximum tool forces occur at the maximum value of θ . At this maximum, $(\sin \theta)/d = [(2R/d) - 1]^{1/2}/R$, and

$$(f_\theta)_{\max} = \frac{2\pi T}{mn} \frac{[(2R/d) - 1]^{1/2}}{R} = \frac{P_R}{m n f} \frac{[(2R/d) - 1]^{1/2}}{R} \quad (18)$$

where $(f_\theta)_{\max}$ is the maximum value of time-averaged tangential tool force. This is an important result, in that it gives a very practical method for estimating maximum tool force.

From these expressions and from Figure 4, it can be seen that maximum tool forces increase as the cutting depth d decreases at a fixed power level (stall torque can be thrown on fewer and fewer teeth). It can also be seen that tool forces are inversely proportional to rotor speed at a fixed power level (power = force \times velocity). Tool forces are, of course, inversely proportional to the number of teeth on the rotor, mn , all other things being equal. These may seem very obvious points, but they are in total contradiction to the intuitive ideas of some equipment operators, who tend to tackle difficult cutting conditions timidly, with minimal cutting depth d and low rotor speed f . During a program that involved testing of a large disc saw in coarse frozen gravel, the cutting teeth were able to survive severe cutting conditions for 15 minutes with $d/R = 0.62$, but when the machine was operated at $d/R = 0.14$, $1/3$ of the cutting teeth were virtually destroyed in 1 minute.

Forces on the rotor axis

Continuing with the analysis of rotor forces, the next major goal is to relate tool forces to forces on the rotor axis, still assuming that tool forces are directly proportional to chipping depth.

Under normal circumstances a symmetrical rotor on a transverse rotation machine has no net side force acting parallel to the axis. The resultant force that acts normal to the rotation axis is, in

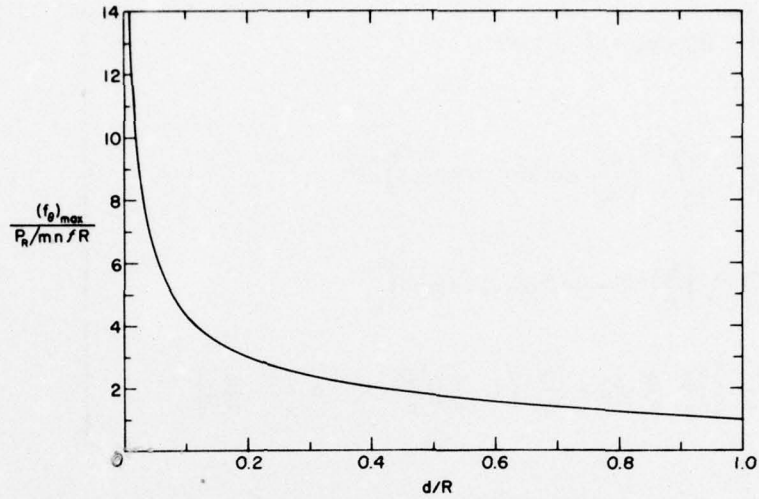


Figure 4. Variation of $(f_{\theta})_{\max}$ with cutting depth d .

general, inclined at some finite angle to the travel direction, and it is convenient to resolve that force into components H and V , which are parallel and normal to the travel direction respectively (Fig. 1).

When the rotor has many tools acting at the same time, as described above, each tool force can be divided by the angular increment over which it acts in order to give force per unit angle, f'_{θ} and f'_{R} . At any angular position θ the unit forces in the tangential and radial directions are

$$f'_{\theta} = \frac{f_{\theta}}{2\pi/mn} = \frac{k_{\theta}}{r} \frac{U}{f} \frac{\sin \theta}{2\pi/m} = f_* \frac{m \sin \theta}{2\pi} \quad (19)$$

and

$$f'_{R} = \frac{f_{R}}{2\pi/mn} = \frac{k_{R}}{r} \frac{U}{f} \frac{\sin \theta}{2\pi/m} = \frac{k_{R}}{k_{\theta}} f_* \frac{m \sin \theta}{2\pi} \quad (20)$$

On each angular increment of the cutting perimeter ($d\theta$) there are radial and tangential forces, f'_{R} and f'_{θ} respectively. These forces can be resolved parallel to, and normal to, the travel direction. For an upmilling rotor, resolution gives:

$$\text{Parallel to travel direction} \quad f'_{R} \sin \theta d\theta + f'_{\theta} \cos \theta d\theta$$

$$\text{Normal to travel direction} \quad f'_{R} \cos \theta d\theta - f'_{\theta} \sin \theta d\theta.$$

The forces on the axis of the upmilling rotor, H and V , are obtained by summing, or integrating, the resolved incremental components:

$$\begin{aligned}
 H &= \int_0^{\theta_m} (f'_R \sin \theta + f'_\theta \cos \theta) d\theta \\
 &= \frac{m}{2\pi} f_* \int_0^{\theta_m} \left(\frac{k_R}{k_\theta} \sin^2 \theta + \sin \theta \cos \theta \right) d\theta \\
 &= \frac{m}{4\pi} f_* \left[\frac{k_R}{k_\theta} (\theta - \sin \theta \cos \theta) + \sin^2 \theta \right]_0^{\theta_m} \\
 &= \frac{F_t}{2} \left[\frac{k_R}{k_\theta} \frac{R}{d} \theta_m - \frac{k_R}{k_\theta} \left(1 - \frac{d}{R} \right) \left(\frac{2R}{d} - 1 \right)^{1/2} + \left(2 - \frac{d}{R} \right) \right]
 \end{aligned} \tag{21}$$

$$\begin{aligned}
 V &= \int_0^{\theta_m} (f'_R \cos \theta - f'_\theta \sin \theta) d\theta \\
 &= \frac{m}{2\pi} f_* \int_0^{\theta_m} \left(\frac{k_R}{k_\theta} \sin \theta \cos \theta - \sin^2 \theta \right) d\theta \\
 &= \frac{m}{4\pi} f_* \left[\frac{k_R}{k_\theta} \sin^2 \theta - (\theta - \sin \theta \cos \theta) \right]_0^{\theta_m} \\
 &= \frac{F_t}{2} \left[\frac{k_R}{k_\theta} \left(2 - \frac{d}{R} \right) - \frac{R}{d} \theta_m + \left(1 - \frac{d}{R} \right) \left(\frac{2R}{d} - 1 \right)^{1/2} \right]
 \end{aligned} \tag{22}$$

in which $\theta_m = \cos^{-1} [1 - (d/R)]$, and k_R/k_θ is a constant, consistent with the assumptions of eq 5-eq 7. H is positive when thrust applied by the machine is in the direction of travel, and V is positive when thrust applied by the machine is downward into the work.

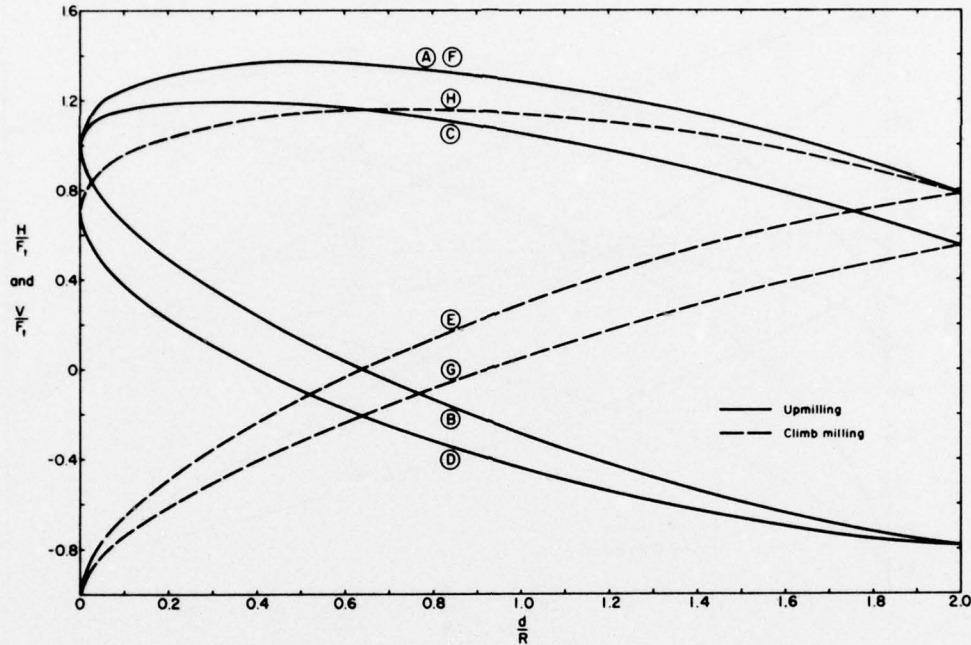
For a climb milling rotor, the resolved incremental forces are:

$$\text{Parallel to travel direction} \quad f'_R \sin \theta d\theta - f'_\theta \cos \theta d\theta$$

$$\text{Normal to travel direction} \quad f'_R \cos \theta d\theta + f'_\theta \sin \theta d\theta$$

and the forces on the axis of the climb milling rotor, H and V , are:

$$\begin{aligned}
 H &= \int_0^{\theta_m} (f'_R \sin \theta - f'_\theta \cos \theta) d\theta \\
 &= \frac{F_t}{2} \left[\frac{k_R}{k_\theta} \frac{R}{d} \theta_m - \frac{k_R}{k_\theta} \left(1 - \frac{d}{R} \right) \left(\frac{2R}{d} - 1 \right)^{1/2} - \left(2 - \frac{d}{R} \right) \right]
 \end{aligned} \tag{23}$$



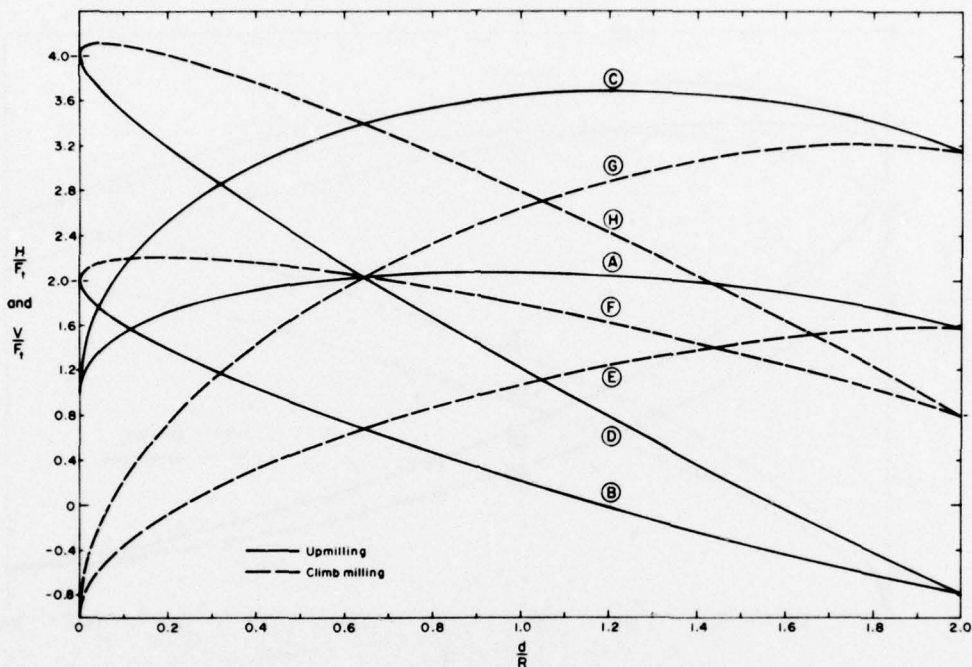
- | | |
|-----------------------------------|------------------------------------------------------------------------|
| A Upmilling, $K = 1.0, H/F_t$ | G Climb milling, $K = 0.7, H/F_t$ |
| B Upmilling, $K = 1.0, V/F_t$ | H Climb milling, $K = 0.7, V/F_t$ |
| C Upmilling, $K = 0.7, H/F_t$ | H is positive when thrust applied by machine is in direction of travel |
| D Upmilling, $K = 0.7, V/F_t$ | V is positive when thrust applied by machine is downward |
| E Climb milling, $K = 1.0, H/F_t$ | |
| F Climb milling, $K = 1.0, V/F_t$ | |

a.

Figure 5. Variation of axle force components H and V with cutting depth d , assuming constant torque. The curves give H and V for upmilling and climb milling with 4 different values of K , assuming f_θ and f_n proportional to ρ .

$$\begin{aligned}
 V &= \int_0^{\theta_m} (f'_R \cos \theta + f'_\theta \sin \theta) d\theta \\
 &= \frac{F_t}{2} \left[\frac{k_R}{k_\theta} \left(2 - \frac{d}{R} \right) + \frac{R}{d} \theta_m - \left(1 - \frac{d}{R} \right) \left(\frac{2R}{d} - 1 \right)^{1/2} \right].
 \end{aligned}
 \tag{24}$$

The results of eq 21-24 are shown graphically in Figure 5, where H/F and V/F are plotted against d/R for four different values of $k_R/k_\theta (= K)$ in both the upmilling and climb milling modes of operation. The influence of the ratio k_R/k_θ is shown more directly in Figure 6, where H/F_t and V/F_t are plotted against $k_R/k_\theta (= K)$ for three values of d/R in the upmilling and climb milling modes.



- | | |
|----------------------------------|--------------------------------------|
| A Upmilling, $K = 2.0$, H/F_t | E Climb milling, $K = 2.0$, H/F_t |
| B Upmilling, $K = 2.0$, V/F_t | F Climb milling, $K = 2.0$, V/F_t |
| C Upmilling, $K = 4.0$, H/F_t | G Climb milling, $K = 4.0$, H/F_t |
| D Upmilling, $K = 4.0$, V/F_t | H Climb milling, $K = 4.0$, V/F_t |

b.

Figure 5 (cont'd). Variation of axle force components H and V with cutting depth d , assuming constant torque. The curves give H and V for upmilling and climb milling with 4 different values of K , assuming f_θ and f_n proportional to d .

Tractive thrust and down thrust

The axle force H , which is parallel to the direction of travel, determines the tractive thrust needed to feed the rotor through the work. In the case of mobile machines, such as large disc saws, wheel ditchers, or drum planers, the available tractive thrust from the carrier vehicle can set the limit of performance for an upmilling rotor. For example, the vehicle may reach its maximum traction (drawbar pull) and spin its tracks before the rotor feed rate is high enough to draw maximum power or to develop maximum torque. In the following discussion, H will be referred to in dimensionless terms in the form of H/F_t , and to give this clearer meaning it will be assumed that F_t is the maximum value that can be developed when the rotor is putting out maximum torque, or is developing its maximum power, i.e.

$$F_t = (F_t)_{\max} = T_{\max}/R = P_{\max}/(2\pi Rf) \quad (25)$$

where P_{\max} is the maximum value of net rotor power.

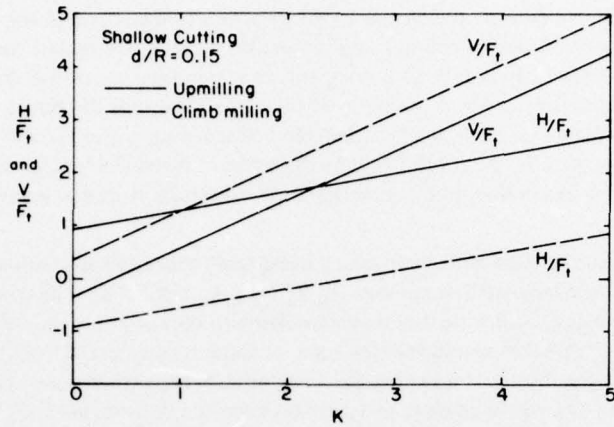
The axle force V , which is perpendicular to the direction of travel and to the work surface, determines the down thrust needed to maintain a given depth of cut d . On mobile machines this down thrust is often provided by hydraulic actuators, and an upper limit to positive down thrust is set by the weight and balance of the whole machine. If the force V exceeds the thrust capability of the actuators or the available reaction, then cutting depth d or forward speed U will have to change in order to limit V . As with H , the force V will be discussed in dimensionless terms as V/F_t , again assuming that F_t is a fixed value set by operation of the machine at its maximum levels of torque and power.

Suppose a machine is fitted with sharp new cutting teeth that develop resultant cutting forces inclined at 45° to their tangential directions: $f_R/f_\theta = k_R/k_\theta = K = 1.0$. The rotor is upmilling, and it is operated so as to utilize the full power available to the rotor, i.e. the forward speed U is kept just below the value that would stall the rotor or cause it to drop off from the peak of the torque curve. With the rotor just touching the work surface, i.e. with d close to zero, the resistance to forward motion H/F_t would be close to 1, and the required downthrust V/F_t would also be close to 1 (Fig. 5a, curves A and B). Setting the rotor deeper into the work would produce an increase in H/F_t (as might be expected intuitively) and a decrease in V/F_t (which may not be obvious). The increase in H/F_t is not very great; a maximum value of $H/F_t = 1.37$ is reached when the rotor is set to a depth equal to about 50% of the effective radius, i.e. at $d/R = 0.5$. The value of H/F_t then falls off again if d is further increased. The vertical thrust V/F_t falls off very significantly as d is increased, and at $d/R = 0.5$, $V/F_t = 0.13$. If d is increased even more, V continues to decrease, dropping to zero at $d/R = 0.64$ and then becoming negative at greater depths. This means that for $d/R > 0.64$ the rotor is tending to pull itself down into the work, and the thrust actuators have to hold it back in order to maintain a fixed cutting depth. In principle, the depth at which V changes from positive to negative is an indication of the value of K for the cutting tools. In some field tests of a rotary drum road planer that were supervised by the writer, the operator of the machine was able to sense the changeover from positive to negative down thrust at a value of $d/R = 0.46$; ignoring the weight of the drum, this implied that K for the cutters was approximately 0.78, a credible value for the sharp-edged tools then in use.

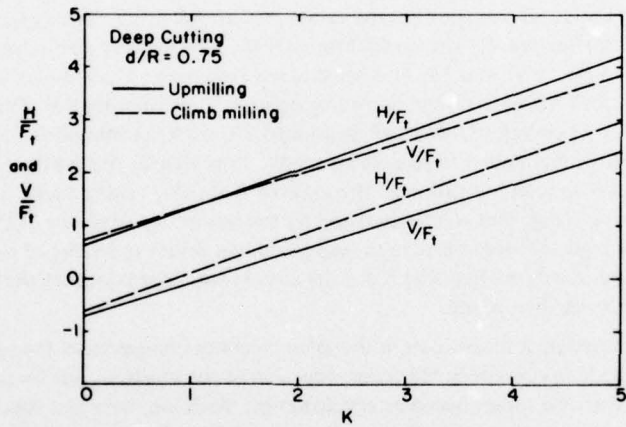
Going back to the original illustration, if the same machine changes from the upmilling mode to the climb milling mode (by reversing the travel direction of the machine, not by reversing the rotation of the rotor), then the forces become very different. With the rotor just touching the surface of the work (d almost zero) the required down thrust would be the same as for the previous case, but the horizontal force would have changed direction to $H/F_t = -1$, i.e. the rotor would be trying to propel the machine (Fig. 5a, curves E and F). Setting the rotor deeper in the work would decrease the self-propelling tendency, and the thrust H would change from negative to positive at a rotor depth of $d/R = 0.64$. Vertical thrust V/F_t would increase to a maximum of 1.37 at $d/R = 0.5$ before slowly decreasing again with further increase in d . In this case the depth at which H changes from positive to negative is an indicator of the effective value of K (pushing or pulling the cutting machine through a dynamometer would give the critical depth). However, deep cutting and aggressive attack in the climb milling mode are usually not very practical due to severe vibrations as the cutters enter the work with maximum chipping depth.

Returning to consideration of the same machine in the upmilling mode, assume that tool wear has increased the value of K (i.e. f_R/f_θ) to 2. At $d = 0$, H/F_t would start at 1.0, as it did with the unworn teeth, but it would increase markedly as d increased, reaching a value of 2 at $d/R = 0.55$ and attaining a maximum value of almost 2.1 at $d/R = 0.9$ (Fig. 5b, curve A). The down thrust V/F_t would start off from a value of 2, i.e. twice as big as the value for the unworn teeth. It would decrease as d increased, falling to a value of $V/F_t = 1.0$ at $d/R = 0.425$, and not changing from positive to negative until reaching a depth of $d/R = 1.18$ (Fig. 5b, curve B).

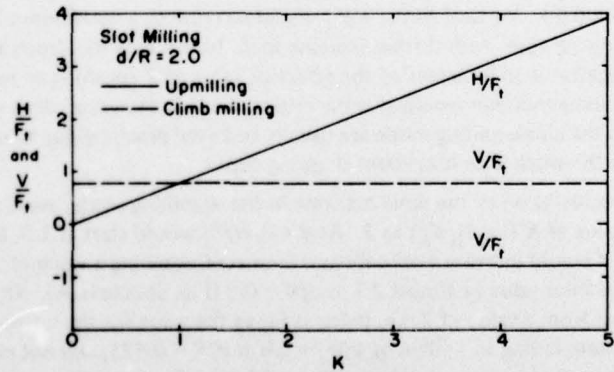
The effect of K , which reflects tool geometry and especially the geometric changes wrought by wear, is shown more directly in Figure 6, where H/F_t and V/F_t are given as functions of K for three



a.



b.



c.

Figure 6. Variation of axle force components H and V with K, assuming constant torque and tool force components proportional to ℓ .

different values of d/R . For *shallow cutting* with $d/R = 0.15$ (Fig. 6a), the effect of K on H is not dramatic. In upmilling, H/F_t increases from 1.28 to 1.64 as K increases from 1 to 2, and in climb milling H/F_t changes from -0.57 to -0.21 as K increases from 1 to 2. There is a much stronger effect on V . In upmilling, V/F_t increases from 0.57 to 1.5 as K changes from 1 to 2, and in climb milling V/F_t increases from 1.28 to 2.2 as K changes from 1 to 2. For *deep cutting* with $d/R = 0.75$ (Fig. 6b), both H and V change by approximately the same amount as K changes. In upmilling, an increase of K from 1 to 2 increases H/F_t from 1.34 to 2.06 and increases V/F_t from -0.9 to $+0.53$. In climb milling, an increase of K from 1 to 2 increases H/F_t from 0.09 to 0.81 and V/F_t from 1.34 to 1.97. For *slot milling* with $d/R = 2.0$ (Fig. 6c), K has no effect on V , but H/F_t increases markedly, a change of K from 1 to 2 increasing H/F_t from 0.78 to 1.57.

On the subject of slot milling, it may be well to draw attention to the side force $\pm V$. From eq 22 and 24, the slot milling side force V_π is

$$V_\pi = \pm \frac{\pi}{4} F_t = \pm \frac{\pi}{4} \frac{T}{R} = \pm \frac{P_R}{8Rf} \quad (26)$$

One research group making experimental studies of slot milling in floating ice sheets completely ignored the existence of a side force, even though that force could (and did) derail the test carriage. Such an oversight would hardly occur after practical experience with a woodworking power router.

Alternative tool force formulations

In the foregoing analysis it is assumed for simplicity that f_R and f_θ are directly proportional to ℓ . However, other formulations can be used if necessary.

An easy refinement is to represent the power relations of eq 1 and 2 by a straight line and a force intercept at $\ell = 0$, such that

$$f_R = A_R + k_R (\ell/r) \quad (27)$$

$$f_\theta = A_\theta + k_\theta (\ell/r) \quad (28)$$

where A_R and A_θ are constants representing the "friction" forces when $\ell = 0$.

Making this substitution, the torque force F_t , previously expressed by eq 13 and 14, becomes

$$\begin{aligned} F_t &= \frac{mk_\theta Ud}{2\pi Rfr} + \frac{mn}{2\pi} A_\theta \cos^{-1} \left(1 - \frac{d}{R} \right) \\ &= \frac{mn}{2\pi} \left[\frac{k_\theta Ud}{rfR} + A_\theta \cos^{-1} \left(1 - \frac{d}{R} \right) \right] \end{aligned} \quad (29)$$

The thrust force on the axle in the travel direction becomes, for upmilling,

$$\begin{aligned} H &= \frac{mk_\theta Ud}{4\pi Rf} \left[\frac{k_R}{k_\theta} \frac{R}{d} \theta_m - \frac{k_R}{k_\theta} \left(1 - \frac{d}{R} \right) \left(\frac{2R}{d} - 1 \right)^{1/2} + \left(2 - \frac{d}{R} \right) \right] \\ &\quad + \frac{mnd}{2\pi R} \left[A_R + A_\theta \left(\frac{2R}{d} - 1 \right)^{1/2} \right] \\ &= \frac{mk_\theta Ud}{2\pi Rf} \phi_1 \left(\frac{d}{R} \right) + \frac{mnd}{2\pi R} \left[A_R + A_\theta \left(\frac{2R}{d} - 1 \right)^{1/2} \right] \end{aligned} \quad (30)$$

where $\phi_1 (d/R)$ is the dimensionless function of eq 21 or 23, as displayed in Figure 4. Putting H in terms of the new value of F_t , as expressed by eq 29:

$$H = F_t \phi_1 \left(\frac{d}{R} \right) - \frac{A_\theta mn}{2\pi} \theta_m \phi_1 \left(\frac{d}{R} \right) + \frac{mn}{2\pi} \frac{d}{R} \left[A_R + A_\theta \left(\frac{2R}{d} - 1 \right)^{1/2} \right]. \quad (31)$$

The reaction force on the axle normal to the travel direction becomes, for upmilling,

$$\begin{aligned} V &= \frac{mk_\theta Ud}{4\pi Rfr} \left[\frac{k_R}{k_\theta} \left(2 - \frac{d}{R} \right) - \frac{R}{d} \theta_m + \left(1 - \frac{d}{R} \right) \left(\frac{2R}{d} - 1 \right)^{1/2} \right] \\ &\quad + \frac{mnd}{2\pi R} \left[A_R \left(\frac{2R}{d} - 1 \right)^{1/2} - A_\theta \right] \\ &= \frac{mk_\theta Ud}{2\pi Rfr} \phi_2 \left(\frac{d}{R} \right) + \frac{mnd}{2\pi R} \left[A_R \left(\frac{2R}{d} - 1 \right)^{1/2} - A_\theta \right] \end{aligned} \quad (32)$$

where $\phi_2 (d/R)$ is the dimensionless function of eq 22 or 24, as displayed in Figure 5. Putting V in terms of the new value of F_t , as expressed by eq 29:

$$V = F_t \phi_2 \left(\frac{d}{R} \right) - \frac{A_\theta mn}{2\pi} \theta_m \phi_2 \left(\frac{d}{R} \right) + \frac{mnd}{2\pi R} \left[A_R \left(\frac{2R}{d} - 1 \right)^{1/2} - A_\theta \right]. \quad (33)$$

The general power relations of eq 1 and 2 are not convenient for analytical solutions, since they lead to integrals that include $\sin^{1/n} \theta$. Numerical solutions are possible, of course, but they have no great merit for exploring the performance characteristics of a machine.

Vehicle traction

When a rotary cutting unit is mounted on a self-propelled vehicle, the forward tractive thrust is usually provided by the net traction of the wheels or crawler tracks. This net traction, which excludes the motion resistance of the wheel or track system, is known in the field of vehicle technology as the drawbar pull D_p ; it gives a measure of the vehicle's reserve capacity to pull, push, or climb slopes. Although the drawbar pull of a vehicle varies considerably with the type of running gear and with the ground conditions, there is an overall linear correlation with vehicle gross weight W , and a dimensionless "drawbar coefficient" C_D is defined as drawbar pull divided by vehicle weight:

$$C_D = D_p/W. \quad (34)$$

On reasonably firm ground surfaces (including dry snow), C_D for track-laying vehicles is typically in the range 0.3 to 0.8, and under very favorable circumstances it can exceed 1.0. On dry soils, firm snow, and pavements, C_D for wheeled vehicles is likely to be in the range 0.1 to 0.6, although higher values are possible under very favorable circumstances.

For a vehicle that carries a transverse-rotation cutting unit, the normal force between the running gear and the ground depends on both the vehicle gross weight W and the vertical thrust force V . Under ideal conditions, where the pitching moment induced by H and V is small, the drawbar pull D_p is

$$D_p = C_D(W - V) \quad (35)$$

noting that V can be positive or negative, as discussed earlier, but following the convention that V is positive when the machine has to thrust downward into the work.

If D_p reaches a limit before rotor torque T or rotor power P_R have reached a limit, then the machine is unable to realize its full performance potential. The amount of power represented by the thrust power $P_H (=UH)$ and by the losses in the running gear (including internal and external motion resistance) is usually quite small, so that there is no great difficulty in supplying adequate power to the tracks. Thus drawbar pull is limited by the tractive efficiency of the running gear, which is expressed by C_D , and a condition for balanced machine design can be written as

$$D_p \geq H \quad (36)$$

or, for a machine that has only a small pitching moment from H and V ,

$$C_D(W - V) \geq F_t \Phi_1(R, d, k_R, k_\theta) \quad (37)$$

where $\Phi_1(R, D, k_R, k_\theta)$ is a function defined by eq 21 or 23, or else by some other similar equation based on different input assumptions. Since V can also be expressed as a multiple of F_t for given operating conditions, as shown in eq 22 and 24, eq 37 can be rewritten as

$$C_D W \geq F_t \Phi_1(R, d, k_R, k_\theta) - C_D F_t \Phi_2(R, d, k_R, k_\theta). \quad (38)$$

This finally becomes, for upmilling:

$$W \geq \frac{F_t}{2} \left[\frac{R}{d} \theta_m \left(\frac{K}{C_D} - 1 \right) - \left(2 - \frac{d}{R} \right) \left(\frac{1}{C_D} + K \right) - \left(1 - \frac{d}{R} \right) \left(\frac{2R}{d} - 1 \right)^{1/2} \left(\frac{K}{C_D} - 1 \right) \right] \quad (39)$$

and for climb milling:

$$W \geq \frac{F_t}{2} \left[\frac{R}{d} \theta_m \left(\frac{K}{C_D} + 1 \right) + \left(2 - \frac{d}{R} \right) \left(\frac{1}{C_D} - K \right) - \left(1 - \frac{d}{R} \right) \left(\frac{2R}{d} - 1 \right)^{1/2} \left(\frac{K}{C_D} + 1 \right) \right] \quad (40)$$

where $K = k_R/k_\theta$.

Conditions 39 and 40 can be evaluated by assuming appropriate values of K and C_d (making allowance for tooth wear and variation of ground conditions), and by substituting $F_t = P_R/2\pi Rf$ (taking maximum power and lowest required rotor speed). Figure 7 shows eq 39 and 40 graphically for two sets of conditions, one where the teeth are sharp and traction is good, and the other where the teeth are worn and traction is fairly poor. This provides a clear indication of the weight penalties incurred by use of poor cutting teeth.

Power/weight ratio

Since gross machine weight is a major determinant of traction capabilities for a self-propelled machine, it is of interest to know something about typical power/weight ratios for existing machines. In Figure 8 the total installed power has been plotted against gross machine weight for a range of machine types, and proportionality lines have been drawn to represent different levels

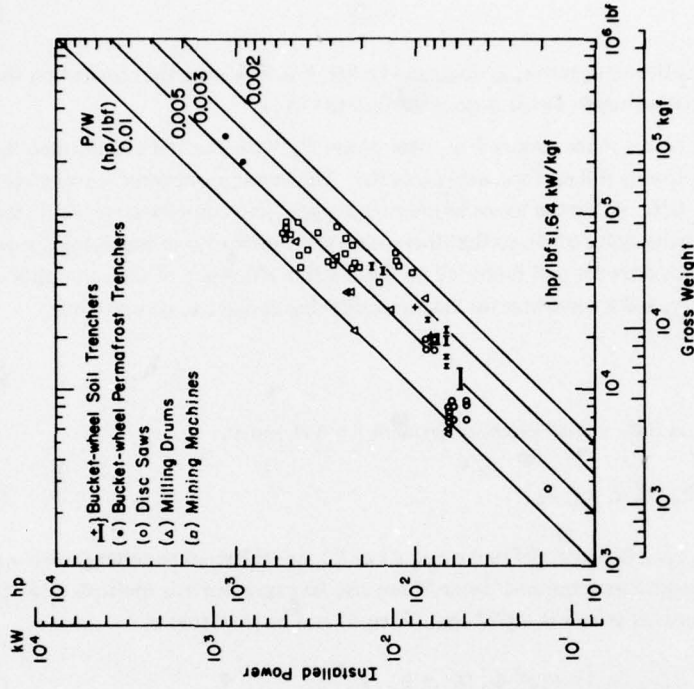


Figure 8. Total installed power plotted against gross machine weight for a variety of existing machines.

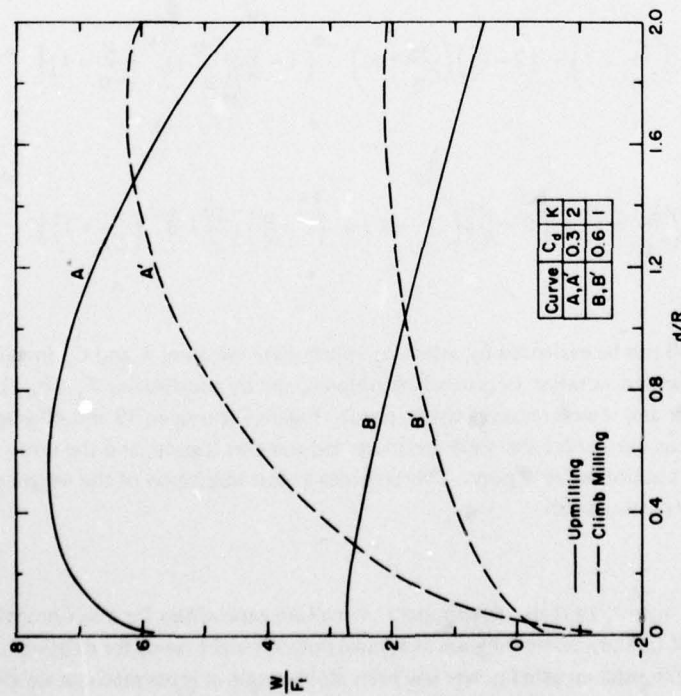


Figure 7. Examples of minimum weight requirements for a carrier vehicle as functions of cutting depth, assuming constant torque and tool force components proportional to λ .

of power/weight ratio. For the equipment covered by the plot, power/weight ratio ranges from about 0.0025 to 0.01 hp/lbf (0.004 to 0.016 kW/kgf). The lower part of the range covers heavy carriers with relatively low-powered cutters, and machines that have a lot of auxiliary equipment, such as the gathering arms and conveyors of some mining machines. The upper limit of the range may be close to the maximum power that can be utilized before traction sets a limit to machine performance.

Weight and balance

With a cutting rotor on a self-propelled vehicle, it is important that the rotor be mounted in such a way that the pitching moment developed by the axle force stays within acceptable limits.

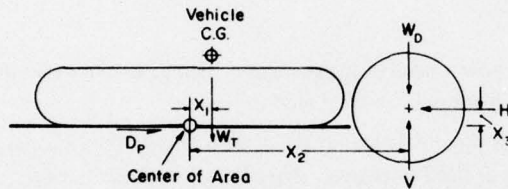


Figure 9. Moments affecting the balance of a mobile machine.

An ordinary unmodified tractor is likely to have its weight W_T distributed over the running gear in such a way that the center of gravity is more or less directly above the center of area of the track (or wheel) system. The static balance might be designed to make the machine slightly nose heavy to compensate for the small moment developed by pulling or pushing. A rotary cutting unit attached to the front or rear of such a tractor immediately disturbs the static balance, and there are further complications when the rotor begins to operate.

Figure 9 gives a simple diagram of forces and moments. The net vertical force on the drum axle is the positive cutting force component V minus the weight of the drum attachment W_D (assuming here that the CG of the complete drum assembly is not far from the drum axle). For the net pitching moment to be zero, the condition is

$$W_T X_1 - (V - W_D) X_2 - H X_3 = 0. \quad (41)$$

When V is positive and greater than W_D , there is clearly an advantage in having the distance X_2 as short as possible. When V is negative (drum pulling itself into the work) or less than W_D , it may be more convenient to eliminate its moment by having reaction shoes or rollers that restrain the drum from further penetration. The moment represented by the third term of eq 41 is small if X_3 is small. This will often be the case in practice; in fact, X_3 can be negative if $d/R > 1$, as it often is during the operation of wheel trenchers. Since $H X_3$ is exactly equivalent to the pulling or pushing loads that crawler tractors are normally designed to cope with, it is unlikely to cause any problems.

In summary, the moment created by H is not likely to cause much difficulty, since tractors are designed to accommodate such a moment. The moment arm X_2 should obviously be kept as short as possible, if only for structural reasons. The effect of positive V is partly offset by the drum weight W_D , and with negative V the drum can be fitted with auxiliary running gear (depth limiters) to provide local reaction against the surface.

Force, torque, speed and power

The energy considerations for cutting machines can be discussed conveniently in terms of the power consumed in various parts of the system. The power for any component or subsystem can often be obtained from the product of force and velocity.

For a single cutting tool at any part of its working stroke, the power P_c is essentially the product of the tangential force component and the tangential velocity, as discussed in Part 4. If U/u_t is small, the tangential tool force is approximately f_θ and the tangential tool speed is approximately u_t , the tangential velocity of the rotor, so that

$$P_c = f_\theta u_t. \quad (42)$$

For the rotor, the net power P_R required for cutting is given by the integrated power consumption for the individual tools:

$$P_R = \frac{mn}{2\pi} u_t \int_0^{\theta_m} f_\theta d\theta = F_t u_t = 2\pi f T. \quad (43)$$

The net cutting power P_R usually includes the power needed to accelerate cuttings and to cycle them against frictional resistance. This is discussed separately in a later section.

The gross power of the cutting rotor includes the power lost in the drive train and the bearings, and the power lost in overcoming air resistance or fluid resistance. These losses are usually easy to measure approximately by running the machine without a cutting load, although bearing friction is actually a function of the cutting load.

The thrust power P_H that is needed to traverse the rotor through the work is

$$P_H = HU \quad (44)$$

where H is the horizontal component of the cutting force and U is the traverse speed. On a self-propelled mobile machine, H sets a minimum requirement for drawbar pull D_p , but there are traction losses that add to the total power required for traction. If the machine has to climb a slope, there is an additional drawbar force of $W \sin \alpha$, where W is gross vehicle weight and α is the slope angle, and thus an additional power requirement of $WU \sin \alpha$. If the vehicle sinks or digs in its tracks when traveling on soft ground, it develops an external motion resistance R , and a corresponding power requirement RU . The wheels or tracks also have an internal rolling resistance, even when the vehicle is traveling on firm, flat ground. The internal rolling resistance can be measured by towing the vehicle on a hard surface, and it can be expressed in terms of a dimensionless resistance coefficient C_r when the resistance force is divided by the vehicle gross weight. The corresponding power loss is thus $C_r WU$. For a tracked vehicle in typical dirty working conditions, C_r might be about 0.1, whereas for a wheeled vehicle it might be only around 0.02.

Specific energy

The specific energy of a cutting machine is defined here as the energy required to cut unit volume of material. Using consistent units, specific energy thus has the same dimensions as stress. In practice, it is rarely convenient to relate energy and volume directly for an operating machine, and the alternative is to work in terms of time derivatives, defining specific energy as power consumption divided by the volumetric cutting rate.

The overall specific energy for a complete machine E_{sT} is based on the total power output of the machine P_T :

$$E_{sT} = P_T / \dot{V} \quad (45)$$

where \dot{v} is the volumetric rate of cutting or excavating, i.e.

$$\dot{v} = UBd. \quad (46)$$

The total power output P_T comprises the rotor power P_R , the thrust power P_H , and the power loss P_L :

$$\begin{aligned} P_T &= P_R + P_H + P_L \\ &= 2\pi fT + UH + P_L. \end{aligned} \quad (47)$$

In this context P_L is the power that does not contribute directly to the cutting process, as described in the section on terminology.

The *process specific energy* E_s for cutting is based on the actual power used for cutting or excavating, excluding P_L :

$$\begin{aligned} E_s &= \frac{P_T - P_L}{\dot{v}} = \frac{P_R + P_H}{\dot{v}} \\ &= \frac{2\pi fT + UH}{UBd}. \end{aligned} \quad (48)$$

In many cases, P_H is much smaller than P_R , and therefore it can sometimes be neglected for practical purposes. This can be demonstrated in the following way:

$$P_H = UH \quad (49)$$

$$P_R = u_t F_t \quad (50)$$

$$\frac{P_H}{P_R} = \frac{U}{u_t} \frac{H}{F_t} = \frac{U}{u_t} \Phi_1(R, d, k_R, k_\theta) \quad (51)$$

where $\Phi_1(R, d, k_R, k_\theta)$ is the function defined by eq 21 or 23, or some similar function. Figure 4 indicates that $H/F_t < 4$. Figure 9 of Part 1 shows u_t mainly in the range 300 to 800 ft/min (1.5 to 4 m/s), and since U is typically in the range 1 to 20 ft/min (0.005 to 0.1 m/s), U/u_t is likely to be small. The net result is that P_H/P_R will usually be in the range 0.01 to 0.1.

In the resulting simplified form

$$E_s \approx \frac{P_R}{\dot{v}} \approx \frac{2\pi fT}{UBd} \approx \frac{2\pi RfF_t}{UBd} \approx \frac{u_t}{U} \frac{F_t}{Bd}. \quad (52)$$

On machines that have electric or hydraulic drive for the rotor and the tracks, fairly close estimates of P_R and P_H can be made by measuring the power delivered to the rotor or track (1) during cutting and (2) during operation of rotor and tracks with the rotor disengaged from the work. The differences give P_R and P_H . With mechanical drive systems only rough estimates can be made, using the rated power output of the engine with estimated efficiency factors and deductions for auxiliary systems driven by the engine. However, for equipment comparisons and for preliminary design, even rough estimates of E_s are often very useful.

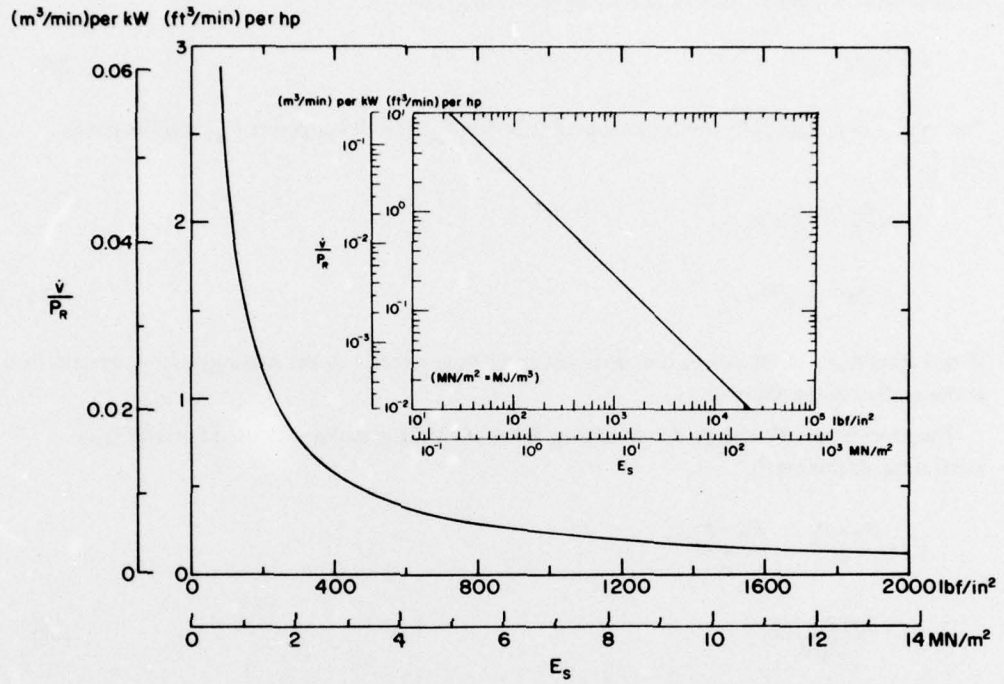


Figure 10. Volumetric cutting rate per unit power as a function of specific energy.

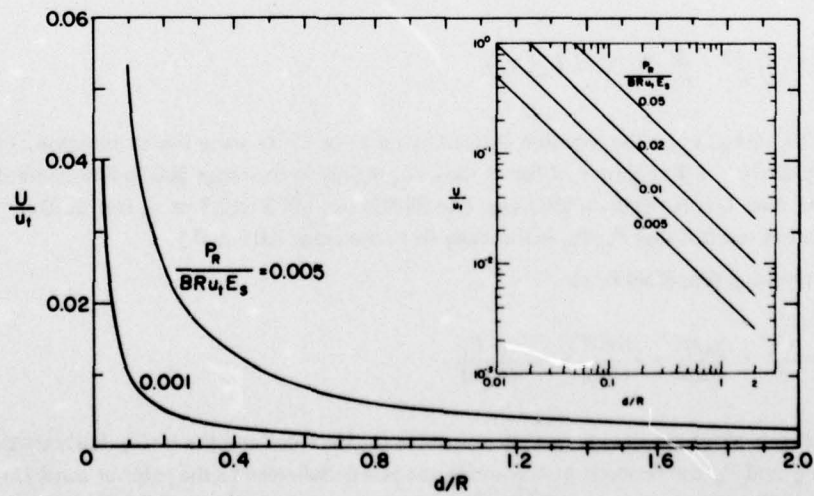


Figure 11. Variation of maximum traverse speed with cutting depth when E_s is held constant.

According to eq 52, the volumetric cutting rate \dot{v} is proportional to specific energy E_s . Figure 10 shows volumetric cutting rate per unit power plotted against specific energy. If E_s can be estimated from test results or machine performance analyses, then production rate or required horsepower can be predicted.

For any given machine working in a given type of material, E_s is likely to vary mainly with chipping depth ℓ . The maximum and mean values of ℓ can be kept constant by varying kinematic parameters in accordance with eq 2 of Part 1, and consequently it ought to be possible to keep E_s reasonably constant. If E_s is kept constant, then eq 52 predicts that traverse speed U will be inversely proportional to rotor depth d , as shown in Figure 11.

Efficiency and performance index

It has already been explained in Part 4 that the specific energy for a single cutting tool can be normalized with respect to the strength of the work material in order to obtain a dimensionless index that characterizes the efficiency of the tool and the cutting mode. The specific energy of a complete rotor is a function of the specific energy for its component tools, but it is not necessarily simply related, since all the tools are cutting to different depths. Nevertheless, a linear correlation between machine specific energy and rock strength can be expected.

In Figure 12 the specific energy E_s has been plotted against uniaxial compressive strength σ_c for a variety of transverse rotation machines working in various materials. These machines include large

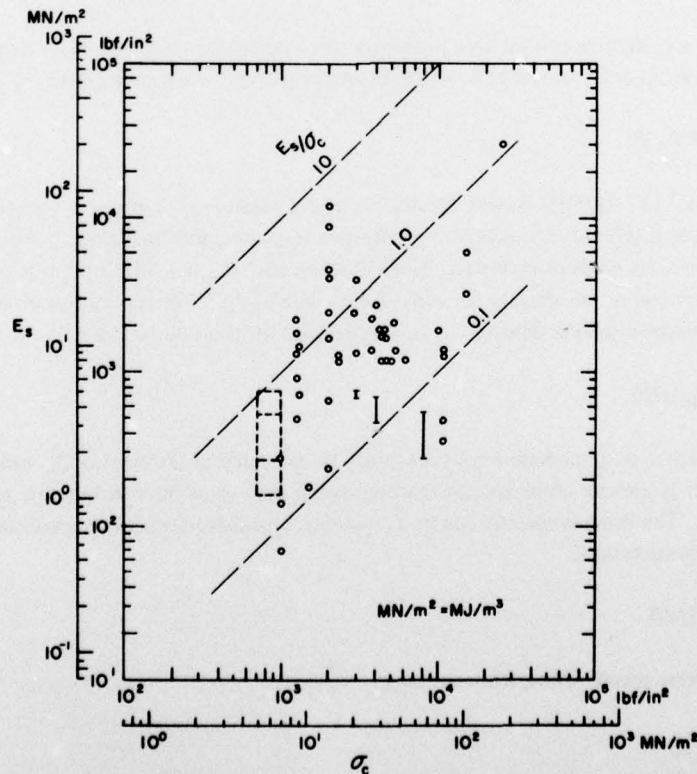


Figure 12. Plot of E_s against σ_c made from performance records of various existing machines. Proportionality lines give values of E_s/σ_c .

disc saws working in concrete and frozen soils, road planers working in concrete, asphalt and frozen soils, special drum machines working in ice and frozen soils, and mining or tunneling machines working in ice, talc, coal, and various sedimentary rocks. Lines are drawn on the graph to represent fixed values of E_s/σ_c .

At first sight there may be a tendency to despair over the high scatter of the data, but in fact the results are both interesting and useful to a designer. The plot indicates that a realistic design goal is to aim for $E_s/\sigma_c \approx 0.1$, and an inspection of the corresponding plot for single drag bit tools provides support for this conclusion (see Fig. 88 of Part 4). It can also be seen that values of E_s/σ_c between 0.1 and 1.0 are readily attainable. If analysis of performance for a machine shows E_s/σ_c approaching 10 (something that is not uncommon in real life), then there is good reason to suspect serious fault in the design or the operating procedure. The plotted values that show E_s/σ_c less than 0.1 are likely to have been obtained under very favorable circumstances, for example in cutting friable coal, well fractured rock, or thermally strained ice.

The dimensionless performance index is useful in preliminary design for estimating power or performance. A value of E_s/σ_c can be assumed on the basis of past performance records, as illustrated in Figure 12 (e.g. assume $E_s/\sigma_c = 0.25$). From the known or measured value of σ_c , this then gives E_s . If production rate \dot{v} has been laid down in some form in the performance specifications, then net rotor power P_R can immediately be estimated. Alternatively, production rate \dot{v} or traverse rate U can be estimated if the net rotor power P_R is given.

Power density

The term *power density* is used here to denote rotor power per unit area of cutting surface. For a transverse rotation drum of radius R , width B , and power P_R , the power density Q is

$$Q = P_R / R \theta_m B \quad (53)$$

where $\theta_m = \cos^{-1} [1 - (d/R)]$. Power density is a useful measure of a machine's power level relative to its dimensions; it is handy for comparing different machines, and for sizing up their probable capabilities in various kinds of materials. Since Q varies with θ_m , i.e. with d/R , it is convenient to also define a nominal power density for some fixed value of θ_m . For typical machines that operate with $d/R < 2$, nominal power density Q_N can be defined for the value $\theta_m = \pi/2$:

$$Q_N = 2P_R / \pi R B. \quad (54)$$

The performance of a machine would obviously be expected to improve as Q_N increased, assuming that dynamic or kinematic limits are not reached, and it may be of interest to relate power density to specific energy. The process specific energy E_s for the rotor is its net power output divided by the volumetric excavation rate:

$$E_s = P_R / U d B \quad (55)$$

where U is traverse speed. Thus, from eq 53-55,

$$\frac{Q}{E_s} = \frac{d}{R} \frac{U}{\theta_m} \quad (56)$$

or,

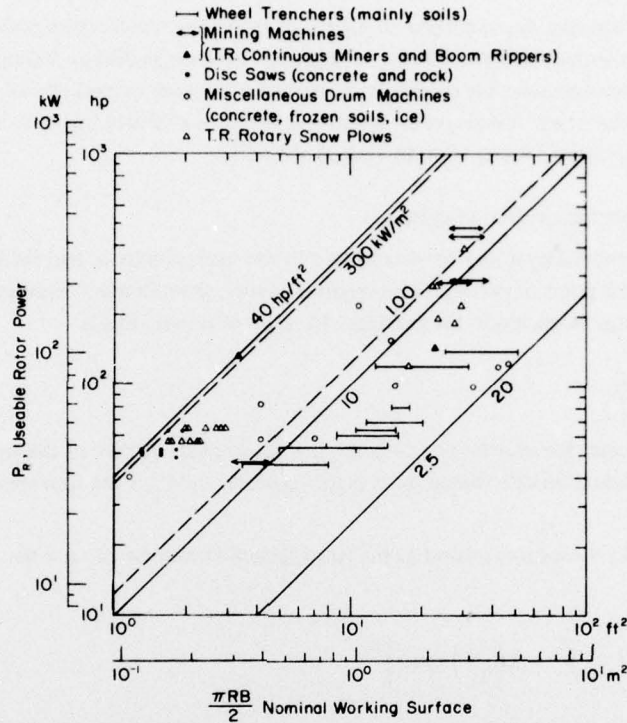


Figure 13. Usable rotor power plotted against the area of one quadrant of the rotor for various existing machines. Proportionality lines give values of nominal power density.

$$Q_N = \frac{2U_N}{\pi} E_s \tag{57}$$

when $\theta_m = \pi/2$, and U_N is the corresponding traverse speed.

Some actual values of nominal power density Q_N are shown for various transverse rotation machines in Figure 13. The highest values, up to 40 hp/ft² (320 kW/m²), are achieved by relatively small machines. In the plot, these are mainly self-propelled disc saws for rock and concrete, and hand-guided snow blowers; one implication is that material properties may not be the power limiting factor in practical design. This impression is reinforced by a comparison of power densities for large rotary snow plows and mining machines.* The data for bucket-wheel trenching machines show a clear tendency for power density to decrease with increasing machine size, perhaps because of structural problems. Very large wheel-ditchers that are being developed for work in permafrost actually have only about the same power density as the smallest ditchers designed for work in unbonded soils. The lowest values shown in the plot are almost down to 2.5 hp/ft² (20 kW/m²), but since these represent machines that are designed to work at small values of θ_m , they tend to be somewhat misleading.

* Snow plow rotors accelerate the cuttings to high tangential velocity, and in some designs the cutting rotor serves as the ejection impeller.

As a matter of interest, wood-cutting circular saws have very much higher power densities than the machines represented in Figure 13; Q_N is typically in the range 200 to 400 hp/ft² (1600 to 3200 kW/m²). Diamond saws for cutting rock and concrete seem to have power densities in the same range as lumber saws. Metal-cutting friction saws have extremely high power densities, in the range 600 to 1200 hp/ft² (about 5000 to 10,000 kW/m²).

Power requirements for ejection of cuttings

The cuttings removed by a tool are accelerated to the tool velocity u , and finally ejected at the tool velocity for the point of exit u_e . This requires energy, the minimum requirements being given by the kinetic energy imparted to the cuttings. In terms of power, this is

$$P_A = \frac{1}{2} \rho \dot{v} u_e^2 \quad (58)$$

where P_A is the power for accelerating cuttings, ρ is the in-place density of the work material, \dot{v} is the volumetric production rate (based on in-place volume), and u_e is the tool velocity at the point of exit.

In general, tool velocity u is related to the rotor tangential velocity u_t and the traverse velocity U by

$$u = u_t \left[1 + \left(\frac{U}{u_t} \right)^2 \pm 2 \left(\frac{U}{u_t} \right) \cos \theta \right]^{1/2} \quad (59)$$

and when U/u_t is small, $u \approx u_t$.

Whether or not P_A is significant relative to rotor power P_R depends largely on the peripheral rotor velocity u_t and the specific energy for the cutting process E_s

$$\frac{P_A}{P_R} = \frac{\frac{1}{2} \rho \dot{v} u_e^2}{E_s \dot{v}} = \frac{\rho u_e^2}{2E_s} \approx \frac{\rho u_t^2}{2E_s} \quad (60)$$

For machines that cut rocks, hard ground, and frozen earth materials ($\rho u_t^2/2E_s$) is typically in the range 10^{-5} to 10^{-2} , so that P_A is not really significant compared to other power losses in the system. However, for high speed machines cutting weak materials, the same would not be true. Wood-working saws and rotary snow plows are two examples. Suppose a rotary snow plow is operating fairly efficiently with $E_s/\sigma_c = 0.3$. If the snow density is 0.4 Mg/m^3 (25 lb/ft^3), σ_c might be about 50 lbf/in.^2 (0.34 MN/m^2), so that E_s would be about 15 lbf/in.^2 (0.1 MN/m^2). With a 4-ft. (1.22 m) diameter drum rotating at 250 rpm, $u_t = 3142 \text{ ft/min}$ (16 m/s). For these numbers ($\rho u_t^2/2E_s$) = 0.49, i.e. the power needed for accelerating cuttings is about 50% of the net cutting power P_R .

Power is also needed to overcome the friction between cuttings and the confining work face. This does not amount to much when radial accelerations are small, of the same order as the gravitational acceleration, but for small high speed rotors it could be significant. Ignoring gravity and assuming that the cuttings scrape over the work face as a coherent mass, the power needed to overcome friction P_F is

$$P_F = \mu \rho \dot{v} \frac{u_t^2}{R} \quad (61)$$

where μ is rock-to-rock friction coefficient, ρ is the in-place density and R is the rotor radius (μ_t^2/R is the radial acceleration). The ratio of friction loss to cutting power is

$$\frac{P_F}{P_R} = \frac{\mu \rho \dot{v} u_t^2 / R}{E_s \dot{v}} = \frac{\mu \rho u_t^2}{E_s R} \quad (62)$$

For typical rock cutting machines, P_F/P_R is likely to be less than 10^{-2} (i.e. P_F less than 1% of P_R), and it could be as little as 10^{-5} . However, for the rotary snow plow described above, P_F might be about 15% of P_R .

Hydrodynamic resistance in underwater cutting

When a rotating drum device or a belt machine is operating underwater, there is additional resistance and power loss caused by the churning of water. When analyzing or designing for underwater work, it is necessary to have at least an approximate estimate of the magnitudes of these effects.

The usual engineering approach to this problem seems to be based on an assumption that each cutter on a drum or belt behaves as an independent bluff body exposed to an otherwise undisturbed flow. This leads to an estimate of hydrodynamic resistance F_w for each tool as

$$F_w = \frac{1}{2} C_d A \rho u_t^2 = \frac{1}{2} C_d h_t w_t \rho u_t^2 \quad (63)$$

where C_d is a drag coefficient of order unity, A is the frontal area of the tool and its mount, ρ is fluid density, and u_t is tool speed. A pair of "effective" values for tool height h_t and tool width w_t have been taken here, such that $h_t w_t = A$. These effective values can also be defined in such a way that tool width w_t is equal to the distance between adjacent parallel cutting tracks w . Following this procedure, the mean shear stress τ_w that is induced by hydrodynamic drag can be written as

$$\tau_w = \frac{1}{2} C_d (h_t/S) \rho u_t^2 \quad (64)$$

where S is the distance between tracking cutters (see Part 3).

The foregoing approach seems reasonable for cases where cutters are spaced far enough apart to be clear of each others' lee eddies or turbulent wakes (the entire problem is, of course, concerned entirely with fully turbulent flow and consequent inertial effects). In broad terms, one might expect eq 64 to be valid when $h_t/S < 0.1$, since the length of the eddy zone behind a bluff body is not likely to be more than ten times the minimum transverse dimension of the body. Where this equation is applicable, the resistance per unit area of belt or drum surface ought to be directly proportional to h_t/S . In cases where tracking cutters are set close together, with h_t/S somewhere between 0.1 and 1.0, the effective turbulent wake will reach back to the following cutter, and reduce its effective height for vortex generation. This interference ought to reduce the shear stress progressively as h_t/S increases, since it is equivalent to reduction of the hydrodynamic "roughness length" that enters into turbulent boundary layer theory. In other words, there ought to be a critical spacing that gives maximum shear stress, and it is probably related quite closely to the length of a turbulent wake.

In a review of fluid resistance in open-channel flow, Rouse (1965)* summarized experimental data for rough boundaries created by sand and by patterns of cubes and spheres. The effective

* Rouse, H. (1965) Critical analysis of open-channel resistance. *Journal of the Hydraulics Division, Proceedings of the American Society of Civil Engineers*, vol. 91, no. HY4, July, p. 1-25.

roughness was expressed as a function of the area concentration of the roughness elements, and it was a maximum at area concentrations from 0.15 (cubes) to 0.25 (spheres). The roughness elements were arranged in repeating "5-spot" patterns, such that there was total coverage of the flow width in each pattern repetition, which is equivalent to the condition $w_t = w$ assumed in the derivation of eq 64. This implies that area concentration is directly proportional to the front-to-back dimension in the direction of flow, which can be labeled s_t for present purposes. Thus the maximum effective roughness, and hence maximum shear stress, occurred when s_t/S was from 0.15 to 0.25. Because the roughness elements were all equidimensional ones, this condition could be rewritten with $s_t/S = h_t/S$. However, if there is any merit to the idea that the length of a turbulent wake determines the limits of interaction, then it might be more consistent to express the critical condition in terms of the depth and length of the *gaps* between roughness elements rather than in terms of the height and spacing of the obstacles when s_t and S are of comparable magnitude (at least for cubic elements).

If the critical condition is written in terms of the height of the roughness element and the gap length (rather than center-to-center spacing), then for equidimensional elements

$$\frac{h_t}{S-s_t} = \frac{s_t}{S-s_t} = \frac{1}{S/s_t-1} \sim 0.15 \text{ to } 0.25. \quad (65)$$

The physical interpretation might be that the length of the eddy zone behind a cubic obstacle is about seven times the obstacle height, and behind a spherical obstacle about four times the diameter.

A more direct study was made recently by Ismail et al. (1977),* who measured water flow resistance as a function of spacing for thin fences set normal to the flow boundary in a conduit. They found that resistance was greatest with $S/h_t \approx 7.5$, i.e. $h_t/S \approx 0.13$.

Drawing some practical conclusions, it can probably be assumed that the effective turbulent wake of an angular obstacle is not more than about eight times the minimum transverse dimension. If it is assumed that $s_t \approx h_t \approx w_t$, it seems a reasonable guess that eq 64 might be applicable up to a value of $h_t/S \sim 10^{-1}$. Effective tool spacings much closer than this are not likely to occur unless there are deep transfer scrolls, scrapers, or buckets, or unless the cutting surface has a sort of sandpaper texture. Lumping together C_d and (h_t/S) in eq 64, a resistance coefficient C_r can be introduced such that

$$\tau_w = \frac{1}{2} C_r \rho u_t^2. \quad (66)$$

The maximum value of C_r is likely to be somewhat less than 10^{-1} , since the critical value of h_t/S is about 10^{-1} and C_d is likely to be less than 1.0 (say 0.6 to 0.9). For water flow in very rough channels, C_r would not be likely to exceed 5×10^{-2} . At the other extreme, the smoothest of natural surfaces have values of C_r about 2.5×10^{-3} for turbulent flow of both air and water.

The power P_w needed to overcome hydrodynamic resistance against the drum or belt surface is

$$P_w = \tau_w u_t A_w = \frac{1}{2} C_r \rho u_t^3 A_w \quad (67)$$

where A_w is the area of the immersed surface. Thus the power density needed to cope with fluid drag Q_w is

* Ismail, E., N. Abd El-Hadi and K.S. Davar (1977) Effects of large roughness on resistance and dispersion in channels. Third National Hydrotechnical Conference, The Canadian Society for Civil Engineering, Laval University, Quebec.

$$Q_w = P_w/A_w = \frac{1}{2} C_r \rho u_t^3. \quad (68)$$

For rock-cutting machines, u_t is typically in the range 1 to 4 m/s (200 to 800 ft/min). With $C_r = 5 \times 10^{-2}$ and the machine operating in fresh water, the corresponding range of Q_w would be 2.5×10^{-2} kW/m² (3×10^{-3} hp/ft²) to 1.6 kW/m² (0.2 hp/ft²). These values of Q_w are based on a surface area that is, in general, greater than the area used for calculating values of power density that relate to the cutting process. The immersed surface area could be two to four times greater than the area of the cutting surface. However, even allowing for this, it is clear from Figure 13 that with low speed drums and belts the fluid drag effects are negligible. At the top end of this speed range, the power requirements for overcoming fluid drag are just about becoming noticeable.

While fluid drag is not much of a problem with typical rock-cutting machines, it can become a significant design factor if high speed rotors are employed, since power increases with the cube of tool speed. High speed circular saws were once considered as aids for icebreaking vessels, and fluid drag was a major consideration.

If high speed disc saws are to be used underwater, the effects of drag on the sides of the disc might have to be considered. Schlichting (1968)* treated the problem of a "free" (i.e. unshrouded) disc creating turbulent motion, the condition for turbulence being $Re = u_t R / \nu < 3 \times 10^5$, where Re is Reynolds number and ν is the kinematic viscosity. The torque T_{ws} created by tangential and radial fluid flow on both sides of the disc is

$$T_{ws} = 0.073 Re^{-1/5} (\frac{1}{2} \rho u_t^2 R^3). \quad (69)$$

The corresponding power dissipation P_{ws} is

$$P_{ws} = T_{ws} \omega = 0.073 Re^{-1/5} (\frac{1}{2} \rho u_t^3 R^2). \quad (70)$$

The power dissipation can also be expressed in terms of a power density by dividing P_{ws} by the total area of both sides of the disc:

$$Q_{ws} = \frac{P_{ws}}{2\pi R^2} = \frac{0.073}{2\pi} Re^{-1/5} (\frac{1}{2} \rho u_t^3). \quad (71)$$

To put some numbers on this, Re first has to be evaluated. The kinematic viscosity of water at +10°C (+50°F) is 1.5×10^{-8} stokes, or cm²/s (1.4×10^{-5} ft²/s). At the lowest tool speed likely to be used for rock-cutting machines, 1 m/s or 200 ft/min, the turbulence condition is met for discs over 0.5 m (1.5 ft) radius.

The power dissipation by drag on the sides of the disc or drum can be compared with the power dissipation by drag on the cutting surface in terms of power densities by comparing eq 68 and 71:

$$\frac{Q_{ws}}{Q_w} = \frac{0.0116 Re^{-1/5}}{C_r} \quad (72)$$

With the lowest applicable value of Re and the highest conceivable values of C_r , Q_{ws}/Q_w is from 1 to 2. With high values for Re (5×10^6 would be a high value for rock-cutting machines), the ratio

* Schlichting, H. (1968) *Boundary-layer theory*. New York: McGraw-Hill, 747 p.

Q_{ws}/Q_w becomes small, so that effects of side shear would only be significant for thin discs, where the side area greatly exceeds the area of the main cutting surface.

Examples

The following worked examples are given in order to illustrate the application of concepts and equations outlined in the report. They are based on actual engineering problems, but have been simplified so as to concentrate on the points raised in this particular report. In real problems the kinematic factors of Part 1 and the tool force aspects of Part 4 have to be considered at the same time, and practical matters of machine morphology, economics, logistics, and so on have to be taken into account.

Example 1

A road planer is removing a 75-mm (2.95-in.) layer of concrete pavement in preparation for re-surfacing on a highway overpass. The transverse-rotation milling drum is 2 m (6.56 ft) long and 1 m (3.28 ft) in diameter. It is powered by internal hydraulic motors, and a check of the hydraulic circuits shows that the drum is drawing 72 kW (96.55 hp) when the machine is traversing at its best speed of 5 m/min (16.4 ft/min). The uniaxial compressive strength of the concrete is 28 MN/m² (4060 lbf/in.²). Calculate the specific energy for this cutting operation, and check the performance index.

The production rate \dot{v} is

$$\begin{aligned}\dot{v} &= UBd = 5 \times 2 \times 0.075 \\ &= 0.75 \text{ m}^3/\text{min} \\ &= 26.48 \text{ ft}^3/\text{min}.\end{aligned}$$

The specific energy E_s is

$$\begin{aligned}E_s &= \frac{P_R}{\dot{v}} = \frac{72 \times 60}{0.75} \quad \frac{\text{kW}\cdot\text{s}}{\text{m}^3} = \frac{\text{kJ}}{\text{m}^3} \\ &= 5.76 \text{ MN/m}^2 \\ &= 835 \text{ lbf/in.}^2\end{aligned}$$

The performance index E_s/σ_c is

$$\frac{E_s}{\sigma_c} = \frac{5.76}{28} = 0.206.$$

Checking this value against Figure 12, the machine appears to be operating quite efficiently by current standards.

Example 2

An upmilling disc saw is to be used for burying telephone and power cables in frozen soils. The saw diameter is 2.1 m (6.89 ft), and the cable trench has to be 0.75 m (2.46 ft) deep. Depth of

freeze in the ground is expected to exceed 1 m (3.28 ft). Maximum working torque for the saw is 12 kN-m (8851 lbf-ft) when the disc is turning at the maximum operating speed of 30 rpm. From previous experience it is known that the cutting teeth undergo rapid initial wear, causing K to increase to a value of approximately 2. The saw is mounted on a light tractor that has pneumatic tires, and the tractor is expected to operate on surfaces that may be lightly snow-covered, icy, or slicked by surface thaw. The gross weight of the rig is 4000 kg (8820 lb). Calculate the traction and vertical reaction requirements for maximum performance, discuss the limiting performance factors and, if necessary, suggest what changes might be made.

During maximum performance operation, the torque force F_t is

$$F_t = \frac{T}{R} = \frac{12 \times 2}{2.1} = 11.43 \text{ kN}$$

$$= 2570 \text{ lbf.}$$

The horizontal and vertical axle forces H and V are calculated from eq 21 and 22, noting that the disc saw is upmilling, $d/R = 0.7143$, $k_R/k_\theta = K = 2$, and $\theta_m = \cos^{-1}(1 - (d/R)) = 1.281 \text{ rad}$:

$$H = 2.053 F_t = 23.46 \text{ kN}$$

$$= 5275 \text{ lbf}$$

$$V = 0.5807 F_t = 6.637 \text{ kN}$$

$$= 1492 \text{ lbf.}$$

The tractor has to develop a drawbar pull of 23.5 kN in order to utilize the available power. Ignoring for the time being the uplift effect of V , the approximate value of the required drawbar coefficient C_D is

$$C_D = \frac{23.46}{4000 \times 9.807 \times 10^{-3}}$$

$$= 0.598 \approx 0.6.$$

If the uplift effect of V is taken into account without immediately considering its moment, the required value of C_D is

$$C_D = \frac{23.46}{4 \times 9.807 - 6.637} = 0.72.$$

These are very high values of C_D and they are not likely to be consistently attainable by rubber tires on slick surfaces.

If the machine is to operate efficiently, drawing full power, then it is necessary to increase the traction or decrease the cutting forces.

Increasing traction is largely a matter of increasing the vehicle weight, and it is probably not feasible to do this to the required extent (the basic vehicle is likely to be carrying ballast already).

An alternative is to lower the cutting forces by increasing the disc speed f and thereby decreasing F_t . Torque T and rotor speed f are inversely related for constant power level P_R :

$$P_R = 2\pi fT = 2\pi RfF_t.$$

If f were to be increased from 30 rpm to 45 rpm, then F_t , H and V would all decrease by a factor of $2/3$. The simple estimate of C_D , which was previously 0.6, would drop to 0.4. The second estimate, roughly taking account of V , would drop to 0.45. The cost of this improvement would be an increase in tool speed u_t , from 3.30 m/s (649 ft/min) to 4.95 m/s (974 ft/min). This might lead to more rapid tool wear, and it would certainly have to be accommodated in the kinematic design (see Part 1) to assure that chipping could be kept within efficient limits. The required modification would probably be an increase of peripheral spacing between tracking cutters.

Because a drawbar coefficient of 0.45 is a bit optimistic for a wheeled vehicle in the conditions described in the question, it would be necessary to strive for every marginal improvement — increase of disc speed, increase of vehicle weight as far as possible, and use of tire chains. A better alternative might be to use a heavier tracked machine.

Example 3

A submarine cutterhead dredge is being designed for burying undersea pipelines in stiff clay. The machine rides on the pipe that is to be buried, cutting a trench by slot milling with a single vertical axis rotor. The rotor diameter is 1.6 m, and the trenching depth is 1.8 m. Proposed rotor speed is 35 rpm, with available power of 150 kW at this speed. With adequate dredge pumps to handle the spoil, the machine is expected to trench at a rate of 150 m/hr in clay that has a shear strength of 100 kN/m². Comment on the proposed power level, and estimate the required traction force and the side force on the pipe.

The power density of the cutterhead, based on the full cutting surface, is

$$Q = \frac{150}{\pi \times 0.8 \times 1.8} = 33.2 \text{ kW/m}^2 = 4.14 \text{ hp/ft}^2.$$

This is comparable to the *nominal* power density of low-powered soil trenchers designed for work on land.

Neglecting for present purposes the power lost by fluid drag, the specific energy corresponding to progress at 150 m/hr is $E_s = 1.25 \text{ MN/m}^2 \text{ (MJ/m}^3) = 181 \text{ lbf/in.}^2$. A correlation between E_s and strength is not presently available for ductile soils, so performance index cannot be checked. It might be noted that σ_c is about twice the simple shear strength (octahedral shear stress = $\sqrt{2}\sigma_c/3$), and by this token E_s/σ_c seems very high for the proposed machine (about 6).

Assuming that the entire rotor power of 150 kW is used for cutting, the torque force F_t is

$$\begin{aligned} F_t &= \frac{P_R}{2\pi Rf} = \frac{150 \times 60}{2\pi \times 0.8 \times 35} \\ &= 51.16 \frac{\text{kW-s}}{\text{m}} = \frac{\text{kJ}}{\text{m}} = \text{kN} \\ &= 11,500 \text{ lbf.} \end{aligned}$$

The torque reaction T that has to be provided by the pipe-riding carriage is RF_t , i.e. 40.9 kN-m or 30,200 lbf-ft.

The required tractive thrust H for moving the cutter ahead under full power is given by eq 21 or 23 as

$$\begin{aligned} H &= K \frac{\pi}{4} F_t = 0.7854 \times 51.16 K \\ &= 40.18 K \text{ kN} \\ &= 9032 \text{ lbf.} \end{aligned}$$

In the case of a soil cutter, K could be less than unity, but a value of $K = 1$ might be taken for design planning.

The side thrust on the pipe V when the cutterhead is developing full power is given by eq 22 or 24, or else by Figure 5, as

$$\begin{aligned} V &= \pm \frac{\pi}{4} F_t = \pm 0.7854 \times 51.16 = 40.18 \text{ kN} \\ &= 9032 \text{ lbf.} \end{aligned}$$

This is a substantial side force that has to be resisted by the flexural rigidity of the pipe, or by some auxiliary stabilizing device.

Example 4

A very big wheel-ditcher is being developed for work in frozen ground, shale, and weathered bedrock. The wheel is 17 ft (5.18 m) in diameter, and its cutting width is 6 ft (1.83 m). The anticipated digging depth for normal operation is 8.5 ft (2.59 m), but it could range between 4.5 ft (1.37 m) and 9.5 ft (2.90 m). Power available to the wheel at the governed rpm of the diesel will be 850 hp (634 kW). The wheel speeds for cutting in hard ground will be 7.5, 9.4 and 11.2 rpm, and there will be no torque limitation other than that of available power. The wheel is to have 20 buckets. The seven cutting teeth on the lip of each bucket are spaced apart, such that the teeth on one bucket track in the gaps left by the preceding bucket, with the tooth pattern repeated on every second bucket (ignore the practical complications of gauge cutters for this example). Calculate and comment on the power density of the machine, and estimate tooth forces for the various working options.

The nominal power density of the wheel, based on cutting to a depth equal to the radius, is

$$\begin{aligned} Q_N &= \frac{2P_R}{\pi RB} = \frac{850}{\pi \times 8.5 \times 6} = 10.6 \text{ hp/ft}^2 \\ &= 85.1 \text{ kW/m}^2. \end{aligned}$$

According to Figure 13, this is appreciably higher than the common range of power densities for typical soil ditchers, and comparable to some mining machines.

The maximum value of the time averaged tooth force is, from eq 18,

$$(f_{\theta})_{\max} = \frac{P_R}{mnf} \frac{(2R/d-1)^{1/2}}{R}$$

In the present case, $m = 14$, $n = 10$, and the total number of teeth $mn = 140$. Note that in this calculation it is the total number of teeth that enters, although the teeth must be set in an orderly array without variation of the peripheral spacing between tracking cutters. The rotor power P_R is 850 hp, or 2.805×10^7 ft-lbf/min.

The estimated tooth forces for the various operating conditions are as follows.

Digging depth (ft)	$(f_{\theta})_{\max}$ (lbf)		
	7.5 rpm	9.4 rpm	11.2 rpm
4.5	5238	4179	3508
8.5	3143	2508	2105
9.5	2793	2228	1870

These are all manageable forces for robust cutting teeth, but force fluctuations caused by the chipping of rocklike material could induce peak values several times higher than the time averaged values estimated above. Force fluctuations depend partly on the compliance of the tool and its mounting.

Example 5

A monopod platform for offshore oil drilling in arctic waters is under consideration. The cylindrical vertical column is to be fitted with a revolving collar and cutting teeth, so that thrust forces from moving ice can be relieved by slot milling. The cutting collar is to be set near the operational waterline with a working depth of 5 m and an effective diameter of 8 m. Maximum ice velocity relative to the structure is expected to be 2 knots, or 1.03 m/s. Calculate: 1) the required cutter power, 2) the magnitude and direction of the maximum cutting force, 3) the variation of cutting force with rotor speed.

The design production rate \dot{v} is given by the product of the cutter diameter ($2R$), the cutter height (B), and the maximum feed rate (U), i.e.

$$\begin{aligned} \dot{v} &= 2R \times B \times U \\ &= 8 \times 5 \times 1.03 = 41.2 \text{ m}^3/\text{s} \\ &= 1455 \text{ ft}^3/\text{s} \\ &= 3233 \text{ yd}^3/\text{min!} \end{aligned}$$

The required net rotor power P_R can be calculated if a good estimate of specific energy E_s can be made, from prior tests, from special tests, or from strength data and assumed values of the performance index E_s/σ_c . For ice, there have been numerous tests of drilling tools, chain and disc saws, and chipping drums, as well as laboratory cutting experiments. It has been shown that with sharp tools chipping deeply, E_s can be less than 100 lbf/in.², or less than 690 kJ/m³. Under ordinary operational conditions, well designed machines have given values of 100 to 500 lbf/in.² (0.69 to

3.45 MJ/m³) when operated properly. By contrast, poorly adapted machines have given values of E_s exceeding 1700 lbf/in.² (over 12 MJ/m³). In the absence of special test data, it will be assumed that a large machine with proper kinematic design (see Part 1) and well maintained cutting teeth can achieve a value of $E_s = 200$ lbf/in.² (1.38 MJ/m³). Taking $\sigma_c = 1200$ lbf/in.², or 8 MN/m², for high loading rates, this value of E_s is equivalent to a performance ratio E_s/σ_c of 0.17, which is not unreasonable.

With $E_s = 1.38$ MJ/m³,

$$\begin{aligned} P_R &= E_s \dot{v} \\ &= 1.38 \times 41.2 \text{ MJ/s} \\ &= 56.9 \text{ MW} \\ &= 76,200 \text{ hp.} \end{aligned}$$

Strictly speaking, this is the net cutting power; the gross power P_T , including hydrodynamic resistance and drive system losses, could well reach appreciably higher values, of the order of 100,000 hp or 75 MW. The power density corresponding to 76,200 hp (56.9 MW) is 113 hp/ft², or 0.91 MW/m². It is questionable whether such high power density is practicable on a very large mechanism.

Real life proposals have featured bigger systems, but assumed smaller power requirements. One scheme called for monopod diameters up to 52 ft (15.9 m), ice thickness (representing pressure ridges) up to 52 ft (15.9 m), and ice velocity between 4½ and 5½ knots (2.3 and 2.8 m/s). The maximum power envisaged was 60,000 hp (44,700 kW), which implies values of E_{ST} of 9 to 11 lbf/in.² (63 to 77 kJ/m³). Assuming that E_s is about 80% of E_{ST} , and taking σ_c for high speed ice cutting as 1200 lbf/in.² (8 MN/m²), the implied value of the dimensionless performance index E_s/σ_c is 0.0061 to 0.0074. At the present state of technology, these are not credible values. The implied power densities (10 to 14 hp/ft², or 76 to 113 kW/m²) are realistic, but the projected performance is mind boggling (\dot{v} up to 56,000 yd³/min).

To calculate thrust forces, a value of K for the cutting teeth has to be assumed, and further assumptions have to be made about the relation between tool force and chipping depth. For this application, it ought to be possible to have aggressive teeth chipping deeply, and it ought to be possible to maintain the teeth in a sharp condition. Thus it will be assumed that tool force is proportional to chipping depth, and that $K = 1$. Accepting these assumptions, the force components on the cutting ring can be read directly from Figure 5a, or calculated from eq 21-24, taking $d/R = 2$:

$$\begin{aligned} \frac{H}{F_t} &= K \frac{\pi}{4} = 0.7854 \\ \frac{V}{F_t} &= \pm \frac{\pi}{4} = \pm 0.7854. \end{aligned}$$

This means that with $K = 1$ the thrust force on the structure will be at 45° to the direction of ice movement. Whether it is angled to right or left depends on the direction of rotation. With higher values of K (i.e. blunter teeth), H would increase, V would be unaffected, and the resultant force would be closer to the direction of ice movement. If the rotor were to be split into two counter-rotating rings, V could be canceled out.

The absolute values of H and V depend on the value of F_t , which varies with rotor speed:

$$F_t = \frac{T}{R} = \frac{P_R}{u_t} = \frac{P_R}{2\pi Rf} = \frac{P_R}{\omega R}$$

$$= \frac{56.9}{4\omega} = \frac{14.23}{\omega} \text{ MN.}$$

when ω is in rad/s. In working man's units:

$$F_t = \frac{76,200 \times 3.3 \times 10^4}{2\pi \times 4 \times 3,28 \times f}$$

$$= \frac{3.05 \times 10^7}{f} \text{ lbf}$$

when f is in rpm. The thrust forces are

$$H = V = 0.7854 F_t = \frac{2.4 \times 10^7}{f} \text{ lbf}$$

$$= \frac{107}{f} \text{ MN.}$$

With a single rotor, the resultant force is $\sqrt{2}H$, or $3.39 \times 10^7/f$ lbf, or $151/f$ MN.

The selection of f depends on a number of factors, including torque capabilities, kinematic factors, hydrodynamic drag, and cutting clearance considerations. Torque should be no great problem with ring gear drive, although torque reaction could create difficulties. Kinematic factors can be handled with proper design (see Part 1). To minimize fluid resistance it is desirable to hold down f , but to clear cuttings it might be necessary to have fairly high speed. On mining and construction machines, u_t (i.e. $2\pi Rf$) is usually between 10^2 and 10^3 ft/min (0.5 and 5 m/s), but at the same time U/u_t is typically of the order of 10^{-2} , and only rarely as high as 10^{-1} .

Taking $U/u_t = 10^{-1}$, $u_t = 2026$ ft/min (10.3 m/s), or 20 knots. The corresponding value of f is 24.6 rpm, and the resultant thrust force for one-way rotation is 1.38×10^6 lbf (689 tons), or 6.14 MN. With $U/u_t = 1$ and $u_t = 202.6$ ft/min (2 knots), f is 2.46 and the resultant thrust force for one-way rotation is 13.8×10^6 lbf (6890 tons), or 61.4 MN. With one-way rotation the torque reaction T is $F_t R$, which amounts to 1.63×10^7 lbf-ft (22.1 MN-m) for $f = 24.6$ rpm and 1.63×10^8 lbf-ft (221 MN-m) for $f = 2.46$ rpm.

The task of maneuvering and holding a dynamically stabilized platform against such forces and torques would seem to be formidable. As a rough rule-of-thumb, tugs and icebreakers develop bollard pulls of about 15 to 30 lbf/hp (90 to 200 N/kW), which suggests that power requirements for a dynamic stabilizing system would be very great.

The reader is invited to repeat the exercise using the values actually proposed for a dynamically stabilized semi-submersible arctic drilling rig. These were: column diameter 26 to 52 ft (7.93 to 15.9 m), ice thickness up to 52 ft (15.9 m), movement velocity $4\frac{1}{2}$ to $5\frac{1}{2}$ knots (2.3 to 2.8 m/s). (Note: it was expected that gross power would be 20,000 to 60,000 hp — see *Oilweek*, 18 November 1974.)